

Evolution of pollen morphology facilitating success of insect pollination: A theoretical and empirical study

著者	Hasegawa Takuya
学位授与機関	Tohoku University
学位授与番号	11301
URL	http://hdl.handle.net/10097/00137185

博士論文

**Evolution of pollen morphology facilitating success of
insect pollination: A theoretical and empirical study**

(虫媒花の送粉成功を促進する花粉形態の
進化に関する理論的・実証的研究)

令和4年度

東北大学大学院生命科学研究科

生態発生適応科学専攻

長谷川拓也

Table of Contents

General Introduction	2
Chapter I. Optimal pollen stickiness to pollinators for maximizing paternal fitness: Increased number of recipient flowers or increased pollen deposition on recipient flowers?	7
Chapter II. Intraspecific variation in morphology of spiny pollen grains along an altitudinal gradient in an insect-pollinated shrub	45
Chapter III. Pollen morphology for successful pollination dependent on pollinator taxa in a generalist plant: Relationship with foraging behavior	74
General Discussion	97
Acknowledgements.....	103
References	105

General Introduction

Insect pollination and pollen morphology

Pollen grains are the carriers of male gametes in seed plants. In angiosperms, 87.5% of species employ animals, whose behavior is outside their control, for transferring pollen between individuals (Ollerton et al., 2011). Since there are multiple routes of pollen loss during animal pollination (Inouye et al., 1994; Minnaar et al., 2019), only a small fraction of pollen in anthers reaches stigmas (Harder and Thomson, 1989; Rademaker et al., 1997). Thus, flowers have a variety of strategies for facilitating pollination via their pollinating partners (e.g., Anderson et al., 2014; Castellanos et al., 2006; Parker et al., 2018).

Pollen grains are morphologically different in many respects at various taxonomic levels despite having the same reproductive function of ovule fertilization (Pacini and Franchi, 2020). Variations in pollen grain size, exines and the amount of pollenkitt (viscous material deposited on angiosperm pollen) have been correlated with pollinator taxa in many studies (e.g., Basso-Alves et al., 2011; Dobson, 1988; Hemsley and Ferguson, 1985; Sannier et al., 2009; Stroo, 2000; Wang et al., 2014). For example, spiny pollen is correlated with fly-pollinated species and smooth-surfaced pollen with beetle-pollinated species in Araceae (Sannier et al., 2009). Although variations in pollen morphology may reflect different optima according to pollinating partners that differ in behavior and morphology, it is still unclear how the interaction between pollen morphology and pollinators affects pollination success and drives the evolution of pollen morphology.

Interactions between pollen morphology and pollinators

Pollen morphology interacts with pollinators in various ways. Pollen spines may influence the probability of anchoring pollen grains to pollinator hairs (Thorp, 1979) while pollenkitt helps pollen adhere to pollinator bodies (Amador et al., 2017; Hesse, 1981; Lin et al., 2013; Pacini and Hesse, 2005). Pollen grain size may dictate the surface area contacting pollinator hairs and

therefore the contact force (Amador et al., 2017). In its interaction with pollinator foraging behavior, pollen morphology may affect the probability of pollen collection from bodies to transport structures by bees. Several studies suggest that pollen grains with large diameters, long spines or large amounts of pollenkitt are less likely to be collected by bees (Hao et al., 2020; Lunau et al., 2015; Vaissière and Vinson, 1994). Thus, the fates of pollen grains should depend largely on interactions of their morphology with pollinators.

Influence of pollen stickiness to pollinators on pollination success

Pollen grains with additional spines or pollenkitt will adhere firmly to pollinator bodies and be less likely to be collected from bodies to transport structures by bees. Such a high level of stickiness to pollinators may reduce pollen loss during transport and increase the amount of pollen deposited on stigmas. In addition, enhanced pollen carryover between flower visits by a pollinator increases the number of flowers receiving pollen grains (Holmquist et al., 2012; Mitchell et al., 2013), thereby relaxing the negative effect of competition among a donor's own pollen grains (Harder and Johnson, 2008).

However, if a stickier pollen grain has a higher cost due to the production of sticking elements such as spines and pollenkitt, there could be the trade-off between the number of pollen grains deposited on stigmas and the number of pollen recipient flowers. Selection on pollen morphology relating to stickiness should operate on the trade-off between them. Moreover, the strength of selection favoring expensive stickier pollen might vary according to pollinator taxa because pollen grooming intensity or foraging areas of pollinators may influence the rate of plant fitness return on the production of additional sticking elements. Therefore, for a better understanding of pollen morphological evolution, it is worth examining how pollen stickiness to pollinators influences the pattern of pollen dispersal and evolves depending on pollinator behavior and morphology.

Intraspecific differentiation in pollen morphology

As well as interspecific variations, there may be intraspecific variations in pollen morphology reflecting differences in pollinators between populations. Lynn et al. (2020) found that pollen grains of *Taraxacum ceratophorum* (Asteraceae) picked up by different taxa of flower visitors were different in quantitative morphological traits, suggesting that pollen morphology facilitating adhesion to insects differs between insect taxa. Therefore, given the prediction that the strength of selection favoring sticky pollen could depend on pollinator taxa, in a generalist plant, pollen morphological traits relating to stickiness could have differentiated between populations having different pollinator assemblages.

Assemblages of pollinators of a generalist plant species can differ among populations at different altitudes, reflecting distributions of animals and plants that are influenced by environmental changes with altitude (Lefebvre et al., 2018; McCabe and Cobb, 2021; Warren et al., 1988). Several studies associated altitudinal variations in floral traits with local pollinator assemblages (e.g., Nagano et al., 2014; Pi et al., 2021). Therefore, altitudinal environmental changes provide opportunities to explore adaptive differentiation in pollen traits of a generalist plant over short distances (Byars et al., 2009; Korner, 2007; Nagano et al., 2014).

Contents of the thesis

In this thesis, I address a question how pollen morphology influences the success of insect pollination and has evolved depending on pollinator taxa. In Chapter I, I theoretically analyzed the effects of pollen stickiness to pollinators on the number of pollen grains deposited on stigmas and the number of flowers receiving pollen grains and examined the optimal level of pollen stickiness to pollinators that differ in parameters on their behavior or morphology. In Chapter II, I empirically tested whether pollen grains of the generalist plant *Weigela hortensis*

(Caprifoliaceae) are different in size, spine phenotypes and amount of pollenkit along an altitudinal gradient. In Chapter III, I tested whether morphology of *W. hortensis* pollen grains facilitating successful pollination depends on pollinator taxa and explains the altitudinal variations. Lastly, I discussed how this thesis extends the knowledge of the function and evolution of pollen morphology in insect-pollinated plants.

Chapter I

Optimal pollen stickiness to pollinators for maximizing paternal fitness: Increased number of recipient flowers or increased pollen deposition on recipient flowers?

Abstract

A plant can sire more seeds by increasing the number of pollen recipient flowers or the amount of pollen deposited on recipient flowers. I theoretically analyzed how pollen stickiness contributes to paternal fitness through changing the pattern of pollen dispersal including both the number of recipient flowers and overall pollen deposition (the overall amount of pollen deposited on recipient flowers) in animal-pollinated plants. I developed a numerical model in which pollen stickiness to pollinators increases with production of expensive materials on pollen surfaces, and a high level of stickiness diminishes the proportions of pollen lost from a pollinator body during a flight and pollen deposited on a stigma during a visit. I found that the number of recipient flowers monotonically increased with increasing pollen stickiness allocation while overall pollen deposition was maximized at a certain amount of stickiness allocation. I demonstrated that evolutionarily stable pollen stickiness attained many recipient flowers at the expense of overall pollen deposition in most cases while it merely favored maximization of overall pollen deposition in all other cases. Sticky pollen evolved if pollinators were highly likely to drop pollen during flights and did not diffuse well. In this situation, the evolutionarily stable pattern of pollen dispersal was acquisition of many pollen recipient flowers rather than maximization of overall pollen deposition. Sticky pollen also evolved if additional sticking elements were moderately effective in increasing the force of adhesion to pollinators. Pollen stickiness has a significant effect on the pattern of pollen dispersal via the extent of pollen carryover, and the results suggest that plants maximize paternal fitness by giving pollen the optimal stickiness, which varies with pollinating partners.

Introduction

Pollen is carried by animals, wind or water and some eventually reaches a stigma. From the perspective of plant male function, a plant can sire many seeds by transferring a lot of pollen to each recipient flower. Alternatively, it can transfer smaller amounts of pollen distributed among a large number of recipient flowers if there is pollen competition for fertilizing ovules of the recipient flowers (Harder and Johnson, 2008). The benefit from wide pollen distribution arises from diminishing returns on pollen deposition on each recipient flower; that is, a donor's pollen deposited on a single stigma faces intense competition for fertilization among the donor's own pollen grains. Thus, it is generally accepted that plants have a variety of strategies for distributing as much pollen as possible to as many recipient flowers as possible.

In angiosperms, 87.5% of species rely on animals, whose behavior is outside their control, for pollination (Ollerton et al., 2011). Hence, for the animal-pollinated plant, the optimal pollen dispersal must be accomplished indirectly via pollinators. One of the major ways to transfer much pollen to recipient flowers might be presentation of much pollen to pollinators. Such mechanisms include increased attraction of pollinators (e.g., Conner and Rush, 1996; Ishii and Sakai, 2001; Kessler et al., 2008), floral shape that is mechanically fitted to pollinating partners (e.g., Aigner, 2004), increased duration of a flower visit (e.g., Harder and Thomson, 1989), and avoidance of stigma-anther interference (e.g., Fetscher, 2001). On the other hand, if many pollinators are available for a flower, it can maximize the overall amount of its pollen delivered to other flowers (overall pollen deposition) by presenting a small amount of pollen to each pollinator because a small amount of pollen on pollinator bodies is not likely to induce grooming and thus relaxes diminishing returns for pollen deposition on stigmas (Harder and Thomson, 1989). Some plants distribute pollen into anthers that sequentially dehisce or expose pollen gradually from an anther to make pollen available to pollinators a little at a time (e.g.,

Castellanos et al., 2006; Harder and Thomson, 1989; Harder and Wilson, 1994; Li et al., 2014; Lloyd and Yates, 1982; Parker et al., 2018; Song et al., 2019). Research on ways to increase the number of pollen recipient flowers is limited, but several studies addressed them in theory. Using a simulation model, Ohashi and Thomson (2009) demonstrated that ‘trapline foragers’, which establish their own foraging areas and repeatedly visit plants within their areas in a roughly fixed order, increase the number of pollen recipient flowers compared to searching foragers. In addition, according to the theoretical framework of Mitchell et al. (2013), if pollen carryover is extensive, for example due to light pollen grooming, the diversity of pollen donors siring seeds within fruits is great, implying that the diversity of flowers receiving pollen from a certain donor is also great.

Although strategies for increasing either overall pollen deposition or the number of pollen recipient flowers have been investigated, no studies have addressed a strategy for maximizing paternal fitness taking both of them into account, to my knowledge. Is there a floral trait that makes a trade-off relationship between overall pollen deposition and the number of recipient flowers? If there is, what pollen dispersal pattern is achieved by the optimal trait to maximize paternal fitness? To address these questions, I analyzed evolution of pollen stickiness to pollinators, which should be selected on the trade-off between overall pollen deposition and the number of recipient flowers.

Pollen morphology is highly diverse at various taxonomic levels and was associated with pollination syndromes in several studies. Sannier et al. (2009) correlated psilate pollen (pollen lacking conspicuous ornamentation) with beetle pollination and echinate (spiny) pollen with fly pollination in Araceae, taking the phylogenetic background into account. Reticulate (net-like) ornamentation, whose function is considered to be storage of pollenkitt (viscous material around a pollen grain), is associated with bird and bat pollination in Phaseoleae (Basso-Alves et al., 2011). Within the genus *Ficus* (Moraceae), there is a weak correlation between

pollen ornamentation and pollination modes (whether the mutual fig wasps are active or passive pollen collectors) (Wang et al., 2014). Dobson (1988) analyzed lipid extracts of pollenkitt from 69 angiosperm species (28 families) and found that pollen of bee-pollinated plants tends to bear oily pollenkitt compared to that of plants pollinated by other animals, including hummingbirds, Lepidoptera and Diptera. Within the genus *Erythrina* (Leguminosae), pollenkitt is more abundant in pollen of passerine-pollinated plants than in pollen of hummingbird-pollinated plants (Hemsley and Ferguson, 1985).

The presence of spines or viscous materials on pollen surfaces is often associated with stickiness to pollinators. It is generally considered that spiny pollen grains are more likely to get caught in the hairy parts of visiting animals (Berger et al., 1988; Vaissière and Vinson, 1994) and that pollenkitt helps pollen adhere to animal bodies (Amador et al., 2017; Hesse, 1981; Lin et al., 2013; Pacini and Hesse, 2005). Thus, pollen grains ornamented with additional sticking elements such as spines and pollenkitt should diminish pollen deposition on a stigma from a pollinator body and enhance pollen carryover and the number of recipient flowers. Moreover, a well-documented role of spines and pollenkitt is resistance against removal from pollinator bodies by pollen grooming (Amador et al., 2017; Konzmann et al., 2019; Lunau et al., 2015; Vaissière and Vinson, 1994). It has been suggested that the presence of spines or pollenkitt mechanically interferes with pollen aggregation processes, which leads to inefficient pollen packing on the corbiculae of honey bees and bumble bees. This effect of sticking elements should contribute to increasing overall pollen deposition on stigmas because a lot of pollen on bee bodies would have a greater chance of being deposited on stigmas than pollen packed on the corbiculae. In addition, light grooming may enhance pollen carryover and thus increase the number of recipient flowers (Holmquist et al., 2012). Given that additional sticking elements around pollen grains affect the number of recipient flowers and pollen deposition on stigmas, variations in pollen morphology may reflect different optima of pollen stickiness (and

consequent patterns of pollen dispersal) which could vary with some factors associated with the pollinating partners, such as intensity of grooming, body surface structure (the ability to hold pollen on their bodies) and flight distance. These factors can be major selection pressures on pollen stickiness allocation because they significantly influence efficiency of pollen loss from pollinator bodies and deposition onto stigmas as well as the potential pollen dispersal area.

In this chapter, I theoretically explored how selection on pollen stickiness operates on the trade-off between the number of recipient flowers and overall pollen deposition and what pollinator characteristics strongly select for stickier pollen. I developed a numerical model in which pollinators carry pollen whose stickiness determines the proportions of pollen deposited on a stigma during a visit and pollen lost from a pollinator body during a flight. Using this model, I examined the evolutionarily stable level of pollen stickiness and the consequent patterns of pollen dispersal, including both the number of recipient flowers weighted on the basis of pollen deposition on individual recipient flowers (the effective number of recipient flowers) and the total amount of pollen deposition on all recipient flowers. I hypothesized that evolutionary stability is achieved by pollen stickiness that attains many recipient flowers (or a lot of overall pollen deposition) without a major reduction in overall pollen deposition (or the number of recipient flowers). To test the hypothesis, I derived the evolutionarily stable level of pollen stickiness and the level of pollen stickiness maximizing overall pollen deposition (or the number of recipient flowers), separately. Then, I compared the number of recipient flowers and overall pollen deposition achieved by the evolutionarily stable level of pollen stickiness to those achieved by the level of pollen stickiness maximizing overall pollen deposition (or the number of recipient flowers). I analyzed dependences of pollen stickiness evolution on five pollinator parameters: the maximum proportions of pollen loss from a pollinator body during a flight and pollen deposition on a stigma during a visit (which appear when no additional resource is allocated to producing sticking elements), two coefficients that describe effectiveness of pollen

stickiness allocation in increasing adhesion force, and the diffusion coefficient that describes stochastic foraging of a pollinator.

Model

General description

A game consisting of a numerical model is presented to examine how the pollen dispersal pattern evolves through selection on pollen stickiness in interactions with pollinating partners. I assume that each plant bears a single cosexual flower. The plant population is infinitely large and has a spatial expanse such that there is on average one individual per unit of space (Fig. I-1). Plants disperse pollen grains throughout the population via pollinators that stochastically forage for many flowers in each bout. Resource allocation to pollen sticking elements enhances pollen force of adhesion to pollinators that diminishes pollen loss from pollinator bodies due to grooming or falling off and pollen deposition from pollinator bodies onto stigmas. The functional relationships between pollen stickiness allocation and the proportions of pollen flows are estimated from the measurements of adhesion force between intact or pollenkitt-free pollen grains and synthetic resin substrates reported by Lin et al. (2013). After pollination, pollen grains on a stigma fertilize ovules produced by the flower. Note that each stigma receives sufficient pollen grains to fertilize all ovules, and the fertilization rate of a donor on a fruit is proportional to its pollen share on the stigma. Self-pollination can be caused by random walks of pollinators; however, I do not assume that selfed seeds suffer reduced viability compared to outcrossed ones. This is because this work focuses on the problem of how selection on pollen stickiness operates on the trade-off between the number of pollen recipient flowers and the overall number of pollen grains deposited on stigmas of recipient flowers (overall pollen deposition), not the problem of whether pollen stickiness contributes to avoidance of self-pollination. Since all individuals are assumed to have equal fitness through their female function,

fitness through male function is calculated as the number of seeds that the focal individual sires after pollen competition throughout the population and then used for a numerical analysis of the evolutionarily stable stickiness allocation. To examine how selection on pollen stickiness operates on the trade-off between the number of pollen recipient flowers and overall pollen deposition, I compared the effective number of recipient flowers between a plant with the evolutionarily stable pollen stickiness and a plant with the pollen stickiness maximizing overall pollen deposition. For the model development, I used Fromhage and Kokko (2010) as a reference for plant population structure and fitness calculations. Variables and parameters are summarized in Table I-1.

Pollen production

Each individual produces a certain number of ovules and has a certain amount of resources that are allocated to pollen production, R . I assume that a stickier pollen grain has a higher cost due to the production of sticking elements such as spines and adhesive materials (e.g., pollenkitt) on its surface. Let $c + s$ be the resource required for a single grain, where c is the fixed resource needed to produce fundamental pollen structures other than sticking elements such as contents and walls and s is the additional resource needed to make sticking elements. Then, the number of pollen grains with stickiness allocation s produced is

$$P(s) = \frac{R}{c + s}.$$

In the following calculations, I scaled R and s by c by setting $c = 1$ without loss of generality.

Relationship between pollen stickiness allocation and the force of adhesion to pollinators

To estimate the functional relationships between pollen stickiness allocation and the proportions of pollen flows from pollinator bodies, I first estimated the functional relationships between

pollen stickiness allocation and increasing adhesion force using the measurements of adhesion force between pollen and synthetic resin substrates by Lin et al. (2013). Let $f(s)$ be the increasing adhesion force of a pollen grain allocated a resource s for sticking elements. Using the data from Lin et al. (2013), I assumed $f(s) = 1 + as^b$, where a and b are positive constants. Here, larger a and b indicate higher effectiveness of stickiness allocation, s , in increasing adhesion force, which may vary with recipient bodies against pollen grains (the properties of b are described in more detail in Appendix I-C). Then, I modeled the shape of $f(s)$ and chose values of a and b that might make sense in animal pollination.

Lin et al. (2013) found that the pollenkitt contents of pollen from two entomophilous plant species, *Taraxacum officinale* (Asteraceae) and *Helianthus annuus* (Asteraceae), are 60 ± 5 wt.% and 30 ± 5 wt.%, respectively. Since there are no data to suggest a relative resource needed to produce pollenkitt per unit mass compared to pollen structures other than pollenkitt such as contents and walls, I supposed that it is within the range of 0.50 to 2.0. Assuming that a resource needed to produce pollen structures other than pollenkitt (c) equals 1, I obtained $s = 0.74$ – 2.9 for *T. officinale* pollen and $s = 0.21$ – 0.86 for *H. annuus* pollen. Lin et al. (2013) also demonstrated that the adhesion force between the pollen of the two species and some substrates became weaker when the pollenkitt on the surfaces was removed by organic solvent: approx. 85% (*T. officinale*) and 61% (*H. annuus*) decreases for polystyrene, approx. 83% (*T. officinale*) and 58% (*H. annuus*) decreases for polyvinyl acetate, and approx. 75% (*T. officinale*) and 45% (*H. annuus*) decreases for polyvinyl alcohol. I do not use the data for hydrophilic silicon substrates because bodies of pollinating insects are assumed to be oily. I converted these data into increases in adhesion force conferred by pollenkitt and used them for the model fitting.

Because I have only two data sets (*T. officinale* and *H. annuus*) for two variables (a and b), there were no differences between the data and the model's prediction. I obtained the following values: $a = 1.9$ – 7.5 and $b = 1.0$ for polystyrene, $a = 1.6$ – 6.4 and $b = 1.0$ for polyvinyl

acetate, and $a = 0.95\text{--}4.1$ and $b = 1.1$ for polyvinyl alcohol. Thus, I analyzed the following model using $a = 0\text{--}10$ as the value associated with effectiveness of stickiness allocation in increasing adhesion force and $b = 1$ for convenience of calculations (the results when $b = 0.5$ or 1.5 are shown in Appendix I-C).

Pollen loss during transport and pollen deposition on stigmas

To describe pollen flow from pollinator bodies, I modified and used the constant carryover model including a term for pollen loss during transport, introduced by Morris et al. (1994). I assume that adhesion force generated by sticking elements around a pollen grain influences the proportions of pollen loss and pollen deposition. However, I do not assume that pollen stickiness is involved in the removal event from anthers because plants have many strategies for presenting pollen gradually to pollinators (e.g., Castellanos et al., 2006; Harder and Thomson, 1989; Li et al., 2014; Lloyd and Yates, 1982; Minnaar et al., 2019; Parker et al., 2018).

Then, I relate pollen stickiness allocation to the proportions of pollen flows. Sticky pollen has the advantage of a low probability of loss from pollinator bodies because its high force of adhesion to pollinator bodies prevents it from being removed by grooming or falling off (Amador et al., 2017; Konzmann et al., 2019; Lunau et al., 2015; Vaissière and Vinson, 1994). Let $\gamma(s)$ be the proportion of pollen lost from a pollinator body during a flight between two flowers. Assuming that $\gamma(s)$ is inversely proportional to the increasing adhesion force, $f(s) = 1 + as^b$, $\gamma(s)$ can be described as follows:

$$\gamma(s) = \frac{\gamma_0}{1 + as^b},$$

where γ_0 is the maximum value of $\gamma(s)$, which appears when $s = 0$ (Fig. I-2a). $\gamma(s)$ decreases with increasing s in a decelerated manner if $0 < b \leq 1$, or first in an accelerated manner and then in a deaccelerated manner if $b > 1$.

At the times of pollinator visits to flowers, sticky pollen is less likely to be deposited on

stigmas of recipient flowers since its high adhesion force would reduce its separation from pollinators. Let $\rho(s)$ be the proportion of pollen deposition on a stigma from a pollinator body at each visit. Assuming that $\rho(s)$ is also inversely proportional to the increasing adhesion force, $f(s) = 1 + as^b$,

$$\rho(s) = \frac{\rho_0}{1 + as^b},$$

where ρ_0 is the maximum value of $\rho(s)$, which appears when $s = 0$ (Fig. I-2a).

Stochastic foraging and pollen dispersal

I suppose that the foraging movement of a pollinator in a period of time consists of many small independent steps in random directions. I place the focal plant individual on the origin of a Cartesian coordinate system in which two coordinates are denoted as x and y and suppose that a pollinator starts at the origin $(x, y) = (0, 0)$ (Fig. I-1). Then, the location of the pollinator at time t , $p(x, y, t)$, is subject to a two-dimensional Gaussian distribution (Codling et al., 2008):

$p(x, y, t) = \frac{1}{4\pi Dt} e^{-\frac{x^2+y^2}{4Dt}}$. This probability density function (PDF) for the pollinator location is the solution of the two-dimensional diffusion equation, $\frac{\partial p(x,y,t)}{\partial t} = D \left(\frac{\partial^2 p(x,y,t)}{\partial x^2} + \frac{\partial^2 p(x,y,t)}{\partial y^2} \right)$,

where D is a positive constant known as the diffusion coefficient. To express the location of the pollinator as the distance from the focal pollen donor, I convert the stochastic variables of the PDF into polar coordinates. Putting $x = r\cos\theta$ and $y = r\sin\theta$ ($0 \leq \theta < 2\pi$), the PDF for the location (r, θ) at time t can be written as $p(r, \theta, t) = p(x, y, t) \times r = \frac{r}{4\pi Dt} e^{-\frac{r^2}{4Dt}}$. Thus, the PDF for the distance r from the focal pollen donor to a pollinator at time t (Fig. I-2b) is

$$\begin{aligned} p(r, t) &= \int_0^{2\pi} p(r, \theta, t) d\theta \\ &= \frac{r}{2Dt} e^{-\frac{r^2}{4Dt}}. \end{aligned}$$

Then, I consider how pollen is dispersed by random-walking pollinators each of which

visits many flowers at fixed time intervals. Let T be the time interval between two consecutive pollinator visits. I assume that each visiting pollinator has enough pollen-adhering spaces and removes a certain number of pollen grains, regardless of their stickiness, from the anthers.

Pollen on pollinator bodies is lost in a proportion $\gamma(s)$ between a departure from a flower and an arrival at the next flower (during the time T) and then deposited on a stigma of the visited next flower in a proportion $\rho(s)$ (Fig. I-1). Thus, the proportion of pollen removed that is deposited on the i th visited flower is

$$d_i(s) = (1 - \gamma(s))^i (1 - \rho(s))^{i-1} \rho(s).$$

I obtain the PDF for pollen removed that is deposited on flowers at a distance r from a donor flower after a bout of pollinator activity (Fig. I-2c),

$$q(s, r) = \sum_{i=1}^{\infty} d_i(s) p(r, iT).$$

Assuming that each donor flower receives a sufficient number of pollinator visits to remove all pollen grains produced, $P(s)$, the total number of pollen grains deposited on stigmas of all recipient flowers after all pollinator visits (i.e., overall pollen deposition; Fig. I-3) is

$$\begin{aligned} Q(s) &= \int_0^{\infty} P(s) q(s, r) dr \\ &= \sum_{i=1}^{\infty} P(s) d_i(s) \\ &= \frac{P(s)(1 - \gamma(s))\rho(s)}{1 - (1 - \gamma(s))(1 - \rho(s))}. \end{aligned}$$

$Q(s)$ does not include the terms for movement of pollinators (D and T) and is calculated without introducing two-dimensional space and a time dimension. However, the assumptions of two-dimensional space and a time dimension are important for the derivation of paternal fitness of a mutant because paternal fitness is determined not only by $Q(s)$ but also by how the pollen

grains are distributed among recipient flowers, or the effective number of pollen recipient flowers. Random-walking pollinators in the two-dimensional plant population would be realistic assumptions that enable me to assess how pollen accumulates on stigmas of recipient flowers depending on their distances from a donor, taking stochastic overlaps of visited flowers into account.

Fitness and evolutionary stability

Here I suppose a mutant with pollen stickiness allocation s' in a population occupied by many wild types with stickiness allocation s and evaluate the fitness of the mutant, $W(s'|s)$. A mutant is at the origin $r = 0$, where a pollinator starts foraging at $t = 0$. Consider that a mutant disperses pollen to a ring-shaped area between the distances from the mutant r_1 and r_2 ($r_2 > r_1$). The number of pollen grains dispersed at any flowers within this area is $\int_{r_1}^{r_2} P(s')q(s', r)dr$. Due to the symmetry between pollen export and import, each of $\pi(r_2^2 - r_1^2)$ wild types within this area receives $Q(s) - \int_{r_1}^{r_2} P(s)q(s, r)dr / [\pi(r_2^2 - r_1^2)]$ competitive pollen grains from the other wild types. Thus, the siring success rate of the focal mutant on this ring-shaped area is

$$\frac{\pi(r_2^2 - r_1^2) \int_{r_1}^{r_2} P(s')q(s', r)dr}{\pi(r_2^2 - r_1^2)Q(s) - \int_{r_1}^{r_2} P(s)q(s, r)dr + \int_{r_1}^{r_2} P(s')q(s', r)dr}.$$

Making the ring infinitesimally narrower ($r_2 \rightarrow r_1$), I obtain the siring success rate on the distance r , $(2\pi r P(s')q(s', r)) / (2\pi r Q(s) - P(s)q(s, r) + P(s')q(s', r))$. Therefore, the siring success of the mutant on the whole population is

$$W(s'|s) = \int_0^\infty \frac{2\pi r P(s')q(s', r)}{2\pi r Q(s) - P(s)q(s, r) + P(s')q(s', r)} dr.$$

I solved this numerically to obtain the evolutionarily stable pollen stickiness allocation, s^* , which satisfies

$$W(s^*|s^*) > W(s'|s^*)$$

for any mutant.

Index of the number of pollen recipient flowers

To obtain an index of the number of pollen recipient flowers, I calculated the effective number of recipient flowers using an inverse Simpson's diversity index (Simpson, 1949). The effective number of recipient flowers equals the number (simply a count) of recipient flowers if pollen is distributed evenly among the recipient flowers but decreases with increasing variation in the number of pollen grains that the plant distributes among the recipient flowers. Simpson's index is $\Lambda = \sum \pi_i^2$, where π_1, π_2, \dots is the proportion of the number of pollen grains distributed to the i th individual among all the grains distributed ($\sum \pi_i = 1$). As stated above, each of $\pi(r_2^2 - r_1^2)$ individuals in a ring-shaped area between the distances r_1 and r_2 from a pollen donor receives $\int_{r_1}^{r_2} P(s)q(s,r)dr / [\pi(r_2^2 - r_1^2)]$ pollen grains. I obtained the effective number of recipient flowers, $N(s)$, as the reciprocal of Λ :

$$\Lambda = \int_0^\infty 2\pi r \left(\frac{P(s)q(s,r)}{2\pi r Q(s)} \right)^2 dr ;$$

$$N(s) = \frac{1}{\Lambda}$$

$$= \frac{4\pi DT(1 - \sigma)^2}{\sigma[1 + \sigma(\log \sigma - 1)]}$$

where $\sigma = 1 - (1 - \gamma(s))(1 - \rho(s))$. Since $N(s)$ monotonically decreases with increasing σ ($0 < \sigma < 1$), $N(s)$ monotonically increases with increasing s in this model (Fig. I-3).

Paternal fitness is expected to increase with both increasing $N(s)$ and increasing $Q(s)$. To examine the evolutionarily stable pattern of pollen dispersal achieved by s^* , I obtained the percentage changes in the number of recipient flowers, which compares $N(s^*)$ with $N(s_Q)$, and

in overall pollen deposition, which compares $Q(s^*)$ with $Q(s_Q)$. Here, s_Q is the pollen stickiness allocation maximizing $Q(s)$ that is obtained analytically. A larger increase in the number of recipient flowers indicates a higher degree of uniform pollen distribution performed with s^* relative to s_Q . A larger reduction in overall pollen deposition indicates a higher degree of inferiority of s^* in overall pollen deposition.

Results and Discussion

Paternal fitness promoted by the number of pollen recipient flowers and overall pollen deposition

It is generally accepted that a plant can sire many seeds by increasing the number of pollen recipient flowers or the amount of pollen deposited on stigmas of the recipient flowers. For the first time, I theoretically demonstrated how pollen stickiness influences the number of recipient flowers and overall pollen deposition (the overall amount of pollen deposited on stigmas of recipient flowers) and determined the optimal pattern of pollen dispersal. As described below, my model revealed that evolutionarily stable pollen stickiness attained many recipient flowers at the expense of overall pollen deposition in most cases while it merely favored maximization of overall pollen deposition in all other cases.

The paternal benefit of distributing pollen to multiple recipient flowers comes from reducing the competition among a donor's own pollen grains on each recipient flower that occurs if the total number of pollen grains on a stigma exceeds the number of ovules produced by the flower (Harder and Johnson, 2008). This way of reducing pollen competition might have received little attention and been poorly studied because the importance of reducing pollen competition has been recognized mainly in the context of sex allocation (Lloyd, 1983; Queller, 1984). An investment in female function in return for a reduction in pollen production increases whole fitness of an individual by reducing competition among its own pollen grains. On the

other hand, I proposed pollen stickiness as a strategy for increasing the number of recipient flowers and found that selection on pollen stickiness operated on the trade-off between the number of recipient flowers and overall pollen deposition. The viewpoint of such a trade-off is important for understanding evolution of pollen morphology relating to stickiness and other male reproductive traits that can make the trade-off.

Pollen stickiness evolution dependent on pollinating partners

In my model, the number of recipient flowers monotonically increased with increasing pollen stickiness allocation although overall pollen deposition was maximized at a certain amount of (including ‘no’) stickiness allocation s_Q (Fig. I-3). Sticky pollen increased pollen carryover rate through diminishing the proportions of pollen loss during a flight and pollen deposition during a visit, which results in an increase in the number of recipient flowers. I examined s^* (the evolutionarily stable pollen stickiness allocation) and s_Q (the stickiness allocation maximizing overall pollen deposition) separately. When $b = 1$, I specially obtain

$$s_Q = \begin{cases} \frac{\gamma_0 \sqrt{[a - (1 - \gamma_0)] / (\gamma_0 + \rho_0)} - (1 - \gamma_0)}{a}, & \text{if } a > \frac{(1 - \gamma_0)[1 - (1 - \gamma_0)(1 - \rho_0)]}{\gamma_0^2} \\ 0, & \text{if } a \leq \frac{(1 - \gamma_0)[1 - (1 - \gamma_0)(1 - \rho_0)]}{\gamma_0^2} \end{cases}$$

(see Appendix I-A for the derivation). Fig. I-4 shows s^* (a–c), s_Q (d–f) and $s^* - s_Q$ (g–i) dependent on γ_0 (the maximum proportions of pollen loss during each flight between two flowers), a (effectiveness of pollen stickiness allocation in increasing adhesion force) and D (the pollinator diffusion coefficient). Here, larger D indicates pollinators that are likely to move long distances in a given time. I did not show the results of changing T (the time interval between two consecutive pollinator visits) because T appears in all equations multiplied by D with the same exponent.

I found that the stickiest pollen ($s^* = 0.450$) evolves if additional sticking elements are

moderately effective in enhancing the force of adhesion to pollinator bodies (i.e., a is moderate; $a = 1.30$) and pollinators do not diffuse well (i.e., D is small; $D = 0.10$) and are highly likely to drop pollen during transport (i.e., γ_0 is extremely large; $\gamma_0 = 0.70$) (Fig. I-4d). Evolution of the stickiest pollen in such situations can be attributed to the combination of two factors: the first is that s_Q was large if γ_0 was large and a was moderate (Fig. I-4e–h), and the second is that stickiness much higher than s_Q tended to be selected to increase the number of recipient flowers if a and D were small (Fig. I-4i–l). s_Q was large if γ_0 was large because the high adhesion force of sticky pollen prevents it from being lost due to intensive grooming or falling off. s_Q was also large if a was moderate because increased stickiness allocation will not lead to a significant increase in the proportion of pollen produced that is deposited on stigmas if a is small, and a small stickiness allocation is sufficient to make that proportion high if a is large. How effective pollen stickiness allocation is in increasing adhesion force might denote how tightly pollinators hold pollen on their bodies. Thus, the condition that a is moderate and D is small might be true for various pollinating insects that are not very hairy, such as some bees, flies. These insects have lower levels of hairiness than butterflies and moths (Roquer-Beni et al., 2020) and move a limited distance as compared to some birds (Krauss et al., 2017). In addition, D would be small when individual pollinators have their own small foraging areas and repeatedly visit a limited number of plants within each area, as observed in bumble bees and hummingbirds (Gill, 1988; Makino et al., 2007; Thomson et al., 1982). I also imagine that γ_0 is large if pollen is groomed intensively or carried on smooth surfaces such as beetles, mouthparts of insects or beaks of birds. Collectively, pollinating animals that select for a very high level of pollen stickiness might include (i) bees which are not very hairy and groom actively, especially if they have their own foraging areas, (ii) beetles, which tend to have hairless bodies, and (iii) other insects carrying pollen on their mouthparts. All three of these pollinators might fulfill the condition that a is moderate, D is small, and γ_0 is large.

Conversely, no sticky pollen ($s^* = 0$) evolved if pollinators were less likely to drop pollen during transport (i.e., γ_0 was small; $\gamma_0 = 0.10$) (Fig. I-4a). γ_0 would be small if pollen is carried on hairy parts of insects that do not groom, or other safe sites (sites on which pollen is hardly lost; Harder and Wilson, 1998) of bees. Even if γ_0 was moderate or larger, $s^* = 0$ if a was extremely small (Fig. I-4a–d). No sticky pollen would be produced if pollen is carried on surfaces too smooth to trap pollen such that additional sticking elements hardly increase the force of adhesion to them. However, since pollenkitt is found in most animal-pollinated pollen and has other roles such as pollinator attraction (Pacini and Hesse, 2005), it would be more reasonable to suggest that the level of pollen stickiness is kept low rather than sticking elements are absent from such pollen.

The effect of ρ_0 (the maximum proportion of pollen deposition on a stigma during each visit) on pollen stickiness evolution was small, but s^* was slightly higher if ρ_0 was small (Fig. I-B1a–d; see Appendix I-B for details).

While I assumed in the model that all pollen produced is removed by pollinators, pollen removal can be incomplete in some situations. If there is a maximum value of the amount of pollen removed from anthers, excess pollen production over that value does not contribute to increasing overall pollen deposition. Thus, if pollen removal from anthers by pollinators is incomplete, stickier and fewer pollen grains should be produced because they have the advantage of being delivered to more flowers.

Effects of pollen stickiness on the number of pollen recipient flowers and overall pollen deposition and the optimal pattern of pollen dispersal

Fig. I-5a–d shows the percentage increase in $N(s)$ (the number of recipient flowers) of s^* compared with s_Q , and Fig. I-5e–h shows the percentage reduction in $Q(s)$ (overall pollen deposition) of s^* compared with s_Q . These percentage changes show the situations in which

paternal fitness was promoted by increasing the number of recipient flowers at the expense of overall pollen deposition.

If additional sticking elements enhance the force of adhesion to pollinator bodies effectively (i.e., a is large) and pollinators do not diffuse well (i.e., D is small), the percentage increase in the number of recipient flowers of s^* compared to when s_Q was large (Fig. I-5a–d). In the former situation, additional sticking elements effectively contribute to increasing the number of recipient flowers, and in the latter situation, paternal fitness is effectively enhanced by increasing the number of recipient flowers because a high probability of revisits to the same few flowers limits the number of recipient flowers. However, a major reduction in overall pollen deposition occurred when a was moderate (Fig. I-5e–h) because more stickiness allocation is necessary for plants to change the rates of pollen flow (Fig. I-2a) and to increase the number of recipient flowers compared to when a was large. The condition that a is large and D is small might be true for various pollinating insects such as some bees, flies, butterflies and moths, which have rough surfaces that trap pollen to varying degrees as compared to some beetles (Faegri and van der Pijl, 1979; Kendall and Solomon, 1973; Willmer, 2011) and move a limited distance as compared to some birds (Krauss et al., 2017). In addition, as stated above, D would be small when individual bumble bees or hummingbirds have their own small foraging areas. My model also predicted that selection on pollen stickiness biased toward the number of recipient flowers would occur if pollen loss during transport is potentially moderate or severe (i.e., γ_0 is moderate or large) (Fig. I-5b–d). In such situations, no small stickiness allocation maximizes overall pollen deposition (Fig. I-4f–h), and a marginal increase in stickiness allocation does not result in a severe reduction in overall pollen deposition (Fig. I-3) because successive increments in stickiness allocation result in progressively smaller decreases in the proportion of pollen flows, $\gamma(s)$ and $\rho(s)$ (Fig. I-2a). I imagine that γ_0 is moderate or larger if pollen is groomed or carried on smooth surfaces such as beetles, mouthparts of insects or beaks

of birds. Collectively, some hairy bees that groom actively might select for pollen stickiness, especially if they have their own foraging areas, and this selection for pollen stickiness greatly increases the number of recipient flowers.

Conversely, plants are likely to produce pollen with a level of stickiness that nearly maximizes overall pollen deposition if pollen is carried on (i) birds (D is large), (ii) hairy insects that do not groom (γ_0 is small), or (iii) other safe sites (Harder and Wilson, 1998) of bees (γ_0 is small). In these pollination situations, except for pollen carried on beaks of birds (i.e., except for cases in which γ_0 is large), no sticky pollen is predicted to evolve.

I found that the percentage increase in the number of recipient flowers ranged from 0.00% to 13.23% (Fig. I-5a–d) and the percentage reduction in overall pollen deposition ranged from –0.46% to 0.00% (Fig. I-5e–h). The percentage reduction in overall pollen deposition was an order of magnitude smaller than the percentage increase in the number of recipient flowers in most cases, implying that plants can increase the number of recipient flowers without a major reduction in overall pollen deposition by producing sticky pollen.

Relationship between pollen traits and stickiness

I assumed that pollen stickiness to pollinators increases with the production of expensive sticking elements on pollen surfaces on the basis of the measurements of adhesion force between intact or pollenkitt-free pollen grains and synthetic resin substrates reported by Lin et al. (2013). On this assumption, the number of pollen recipient flowers monotonically increased with increasing pollen stickiness allocation while overall pollen deposition was maximized at a certain amount of stickiness allocation (Fig. I-3). On the other hand, as for pollen diameter, an intermediate trait value could maximize the force of adhesion to pollinators, reflecting the mechanical fit between pollen size and pollinator hair spacing (Amador et al., 2017). If an intermediate trait achieves the greatest force of adhesion to a pollinator body, the model will

predict that the number of pollen recipient flowers is maximized by the intermediate trait achieving the greatest adhesion force. Since overall pollen deposition will be maximized by a trait that has a lower cost than does the trait maximizing pollen recipient number, an optimal trait will fall between the two traits. An optimal trait should be closer to the trait achieving the greatest adhesion force under the conditions where stickier pollen was predicted to evolve (Fig. I-4a–d).

Unfortunately, the effects of pollen stickiness on pollen flow have been poorly investigated. Further studies on direct quantification of the flow of pollen varying in traits could improve my model predictions by fixing the functions that link pollen stickiness allocation to the rates of pollen flow, $\gamma(s)$ and $\rho(s)$, more accurately (Fig. I-2a).

Conclusions

Male reproductive traits evolve depending on returns on both increased number of pollen recipient flowers and increased overall pollen deposition. Pollen stickiness has a significant effect on the pattern of pollen dispersal via the extent of pollen carryover, and the results suggest that plants maximize paternal fitness by giving pollen the optimal stickiness that varies with pollination partners. The strength of selection favoring stickier pollen should depend on pollinator characteristics. Pollen stickiness should be one of the few strategies operating after removal from anthers while other possible strategies such as pollen presentation may operate at the removal phase. Future studies that correlate evolution of these strategies operating at different phases should bring a broader understanding of pollen dispersal strategies.

Appendices

Appendix I-A. Derivation of s_Q when $b = 1$

When b (the exponential coefficient denoting effectiveness of stickiness allocation in increasing

adhesion force) equals one, I can analytically obtain s_Q (the stickiness allocation maximizing the total amount of pollen deposited on stigmas, $Q(s)$). Solving $\partial Q(s)/\partial s = 0$ for $s (\geq 0)$ gives

$$s = s_0 = \frac{\gamma_0 \sqrt{[a - (1 - \gamma_0)] / (\gamma_0 + \rho_0)} - (1 - \gamma_0)}{a}, \quad \text{if } s_0 \geq 0,$$

where a is the linear coefficient denoting effectiveness of stickiness allocation, γ_0 is the maximum proportion of pollen loss, and ρ_0 is the maximum proportion of pollen deposition. Since $Q(0) = R(1 - \gamma_0)\rho_0/[1 - (1 - \gamma_0)(1 - \rho_0)] > 0$ and $Q(s) \rightarrow 0$ as $s \rightarrow \infty$ (R is the resource allocated to pollen production), $Q(s)$ with $s \geq 0$ has a maximum at $s = s_0$ if $s_0 > 0$ or at $s = 0$ if $s_0 \leq 0$. Therefore, solving $s_0 > 0$ (and $s_0 \leq 0$) for a , I obtain

$$s_Q = \begin{cases} \frac{\gamma_0 \sqrt{[a - (1 - \gamma_0)] / (\gamma_0 + \rho_0)} - (1 - \gamma_0)}{a}, & \text{if } a > \frac{(1 - \gamma_0)[1 - (1 - \gamma_0)(1 - \rho_0)]}{\gamma_0^2} \\ 0, & \text{if } a \leq \frac{(1 - \gamma_0)[1 - (1 - \gamma_0)(1 - \rho_0)]}{\gamma_0^2} \end{cases}$$

Appendix I-B. Effect of ρ_0 on pollen stickiness evolution

Fig. I-B1 shows s^* (the evolutionarily stable pollen stickiness allocation; a–d), s_Q (the stickiness allocation maximizing the total amount of pollen deposited on stigmas; e–h) and $s^* - s_Q$ (i–l) dependent on γ_0 (the maximum proportion of pollen loss), a (effectiveness of stickiness allocation) and D (the diffusion coefficient) if ρ_0 (the maximum proportion of pollen deposition) was small (= 0.010). If ρ_0 was small (Fig. I-B1a–h), s^* and s_Q tended to be larger and had a similar dependence on γ_0 , a and D compared to when ρ_0 was large (= 0.10; Fig. I-4a–h). If pollen on pollinator bodies remains there for a long time without deposition on stigmas (i.e., ρ_0 is small), sticky pollen is advantageous for increasing overall pollen deposition because its high force of adhesion to pollinator bodies allows the possibility for deposition on stigmas on future visits. In addition, if ρ_0 was small (Fig. I-B1i–l), the difference between s^* and s_Q was almost the same as when ρ_0 was large (Fig. I-4i–l).

Fig. I-B2 shows the percentage increase in the number of pollen recipient flowers (a–d) and the percentage reduction in overall pollen deposition (e–h) dependent on γ_0 , a and D if ρ_0 was small. Both percentage changes were almost the same as when ρ_0 was large (Fig. I-5).

Comparing the cases where ρ_0 was large (Figs. I-4 and I-5) or small (Figs. I-B1 and I-B2), there were only small differences in the dependences of s^* and s_Q on γ_0 , a and D and the percentage changes in the number of recipient flowers and overall pollen deposition. This may be explained mainly by the following two reasons. First, the value of ρ_0 is not directly related to the amount of pollen that is excluded from further dispersal due to grooming or loss during flight. Thus, the effect of ρ_0 on pollen stickiness evolution may be smaller than that of γ_0 . Second, ρ_0 is assumed to be smaller than γ_0 , as I set it. For example, in the *Echium-Bombus* system, approx. 0.15% of pollen on a *Bombus* body was deposited on a stigma during a visit, and approx. 6.1% of pollen on a *Bombus* body is lost during a flight between two flowers or on floral parts other than a stigma (Rademaker et al., 1997).

Nonetheless, my model predicted that somewhat stickier pollen evolves if ρ_0 was small (Figs. I-4a–d and I-B1a–d). ρ_0 would be small due to a short duration of a pollinator visit per flower (Castellanos et al., 2003).

Appendix I-C. Effect of b on pollen stickiness evolution

Although the model fitting shows that b (the exponential coefficient denoting effectiveness of stickiness allocation in increasing adhesion force) is approximately equal to one, it could vary from one according to characteristics of pollinators' body surfaces. The properties of b are summarized as follows:

- (i) If b is larger, the force of adhesion to pollinator bodies increases with increasing s in a more accelerated manner.
- (ii) If $0 < s < 1$, the force of adhesion to pollinator bodies is smaller if b is larger. If $s > 1$, it is

greater if b is larger.

Unlike in the case of $b = 1$ (see Appendix I-A), I numerically obtained s_Q (s maximizing $Q(s)$ with $s \geq 0$) when $b \neq 1$.

Figs. I-C1 and I-C3 show s^* (a–d), s_Q (e–h) and $s^* - s_Q$ (i–l) dependent on γ_0 , a and D if $b = 0.5$ or 1.5 , respectively. There was a clear interaction among a , b and γ_0 . If a or γ_0 was small, s^* and s_Q were smaller if b was larger (Figs. I-4, I-C1 and I-C3). This is because, if $0 < s < 1$, the force of adhesion to pollinator bodies is smaller if b is larger. On the other hand, if both a and γ_0 were large, s^* and s_Q were larger if b was larger (Figs. I-4, I-C1 and I-C3). If pollen is likely to be lost from pollinator bodies, there is a great advantage of decreasing $\gamma(s)$ (the proportion of pollen loss) by increasing pollen stickiness. In addition, if a is large, the effect of larger b in accelerating the increase in adhesion force with increasing s is significant. As a result of these two factors, s^* and s_Q increased with increasing b if both a and γ_0 were large.

If $b = 1.5$, s_Q changed drastically at a certain value of a (Fig. I-C3g, h). If $b > 1$, $Q(s)$ with $s \geq 0$ can have two maxima at $s = 0$ and elsewhere (Fig. I-C5). The reason for this curve shape can be roughly understood from the shape of $\gamma(s)$, which decreases with increasing s , first steadily, then rapidly, and again steadily, if $b = 1.5$ (Fig. I-2a). The parts of decreasing $Q(s)$ almost correspond to the parts of steadily decreasing $\gamma(s)$, and the part of increasing $Q(s)$ almost corresponds to the parts of rapidly decreasing $\gamma(s)$. In addition, if a is large, the maximum at $s \neq 0$ is larger than the maximum at $s = 0$ because $\gamma(s)$ decreases effectively with increasing s . Because the larger maximum switches at a certain value of a , s_Q also changed drastically at the same value of a . Hence, if $b = 1.5$, $s^* - s_Q$ were very large (up to approx. 0.87) at the value of a which was slightly smaller than that switching s_Q (Fig. I-C3k, l).

Figs. I-C2 and I-C4 show the percentage increase in the number of pollen recipient flowers (a–d) and the percentage reduction in overall pollen deposition (e–h) dependent on γ_0 , a and D if $b = 0.5$ or 1.5 , respectively. Similar to $s^* - s_Q$, both percentage changes were very

large (up to approx. 47.21% and approx. -12.36%) at the value of a which was slightly smaller than that switching s_Q if $b = 1.5$ (Fig. I-C4c, d, g, h).

The effect of b on pollen stickiness evolution was significant. In particular, if $b > 1$, $Q(s)$ with $s \geq 0$ can have two maxima at $s = 0$ and elsewhere (Fig. I-C5), and s^* changed drastically depending the values of γ_0 , a and D (Fig. I-C3a–d). However, it might make sense to consider that the force of adhesion to pollinator bodies increases with increasing s in a roughly linear manner ($b \approx 1$) or in a decelerated manner ($0 < b < 1$) unless sticking elements around pollen surfaces work cooperatively as glue to pollinator bodies.

Table I-1. Symbols used in the model

Symbol	Determinant	Definition [Dimension]
R	Plant	Resources allocated to pollen production
c	Plant	Fixed resources needed to produce fundamental pollen structures other than sticking elements
s	Plant	Additional resources needed to produce sticking elements
P	Plant	Number of pollen grains produced (per capita)
f	Both	Increasing adhesion force of a pollen grain due to added sticking elements
a	Pollinator	The linear coefficient denoting effectiveness of stickiness allocation in increasing adhesion force
b	Pollinator	The exponential coefficient denoting effectiveness of stickiness allocation in increasing adhesion force
γ	Both	The proportion of pollen lost from a pollinator body during a flight between two flowers
γ_0	Pollinator	The maximum value of γ
ρ	Both	The proportion of pollen deposited on a stigma from a pollinator body at a single visit
ρ_0	Pollinator	The maximum value of ρ
x, y	—	The coordinates in a 2D Cartesian coordinate system [length]
r	—	The radial coordinate in a polar coordinate system: a distance from a focal donor flower [length]
θ	—	The angular coordinate in a polar coordinate system [rad]
t	—	Time having elapsed since a pollinator started from a focal donor flower [time]
D	Pollinator	The diffusion coefficient of a pollinator random walk [length ² /time]
T	Pollinator	The time interval between two consecutive pollinator visits [time]
d_i	Both	The proportion of pollen removed that is deposited on the i th visited recipient flower
q	Both	The probability density function for pollen removed that is deposited on flowers at a distance r from a donor flower after all pollinator visits
Q	Both	The total number of pollen grains deposited on stigmas of all recipient flowers after all pollinator visits (i.e., overall pollen deposition)
N	Both	The effective number of pollen recipient flowers
s'	Plant	Allocation for sticking elements of a mutant
s^*	Plant	Evolutionarily stable allocation for sticking elements
W	Both	Paternal fitness of a focal donor flower

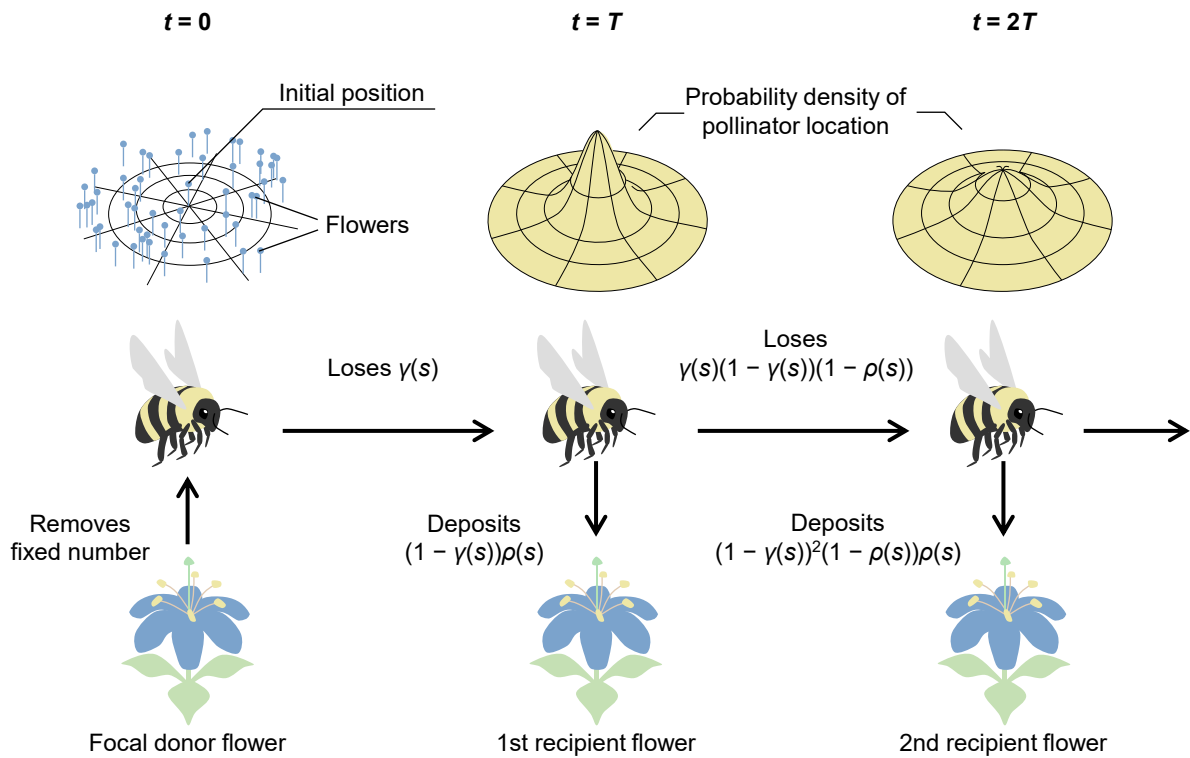


Fig. I-1. Schematic illustrations of a plant population, pollinator movement and pollen dispersal. The plant population is two-dimensional and infinitely large. A pollinator removes a fixed number of pollen grains from a focal donor flower at time $t = 0$ and then forages for many flowers through a random walk at fixed time intervals T . Pollen on a pollinator body is lost in a proportion $\gamma(s)$ during two consecutive visits (during the time T) and then deposited on a stigma of the visited flower in a proportion $\rho(s)$.

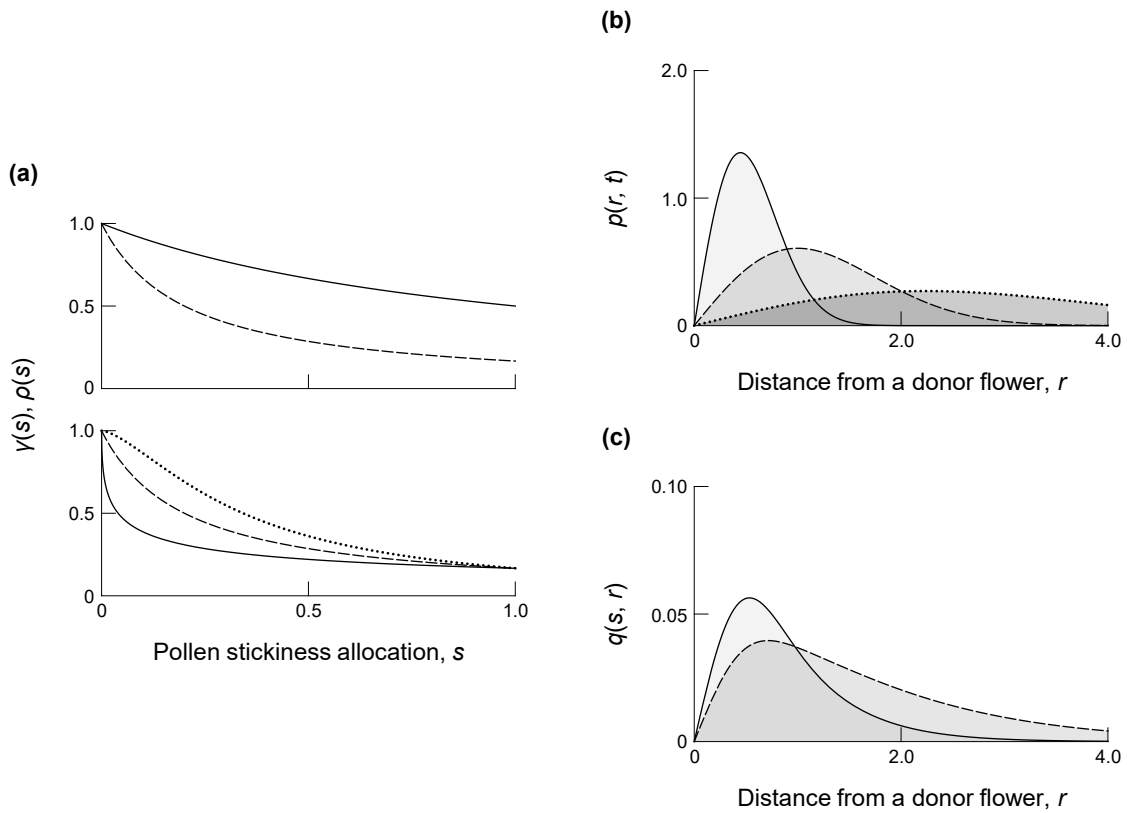


Fig. I-2. (a) The effects of pollen stickiness allocation on the proportion of pollen loss from a pollinator body during a flight between two flowers, $\gamma(s)$, and the proportion of pollen deposition from a pollinator body on a stigma of a visited flower, $\rho(s)$. The upper panel shows the dependence on a : $a = 1.0$ (a solid line), $a = 5.0$ (a dashed line), and $b = 1.0$. The bottom panel shows the dependence on b : $b = 0.50$ (a solid line), $b = 1.0$ (a dashed line), $b = 1.5$ (a dotted line), and $a = 5.0$. γ_0 or $\rho_0 = 1.0$ in both panels. (b) The probability density for a pollinator at a distance r from a donor flower: $t = 1.0$ (a solid line), $t = 5.0$ (a dashed line), and $t = 25.0$ (a dotted line). $T = 1.0$ and $D = 0.10$. (c) The probability density for pollen removed that is deposited on flowers at a distance r from a donor flower: $s = 0.100$ (a solid line) and $s = 1.00$ (a dashed line). $\gamma_0 = 0.50$, $\rho_0 = 0.050$, $a = 5.0$, $b = 1.0$, $T = 1.0$, and $D = 0.10$.

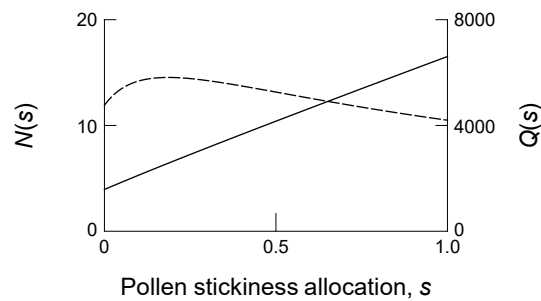


Fig. I-3. The effects of pollen stickiness allocation on the number of pollen recipient flowers, $N(s)$, and overall pollen deposition (the overall amount of pollen deposited on stigmas of the recipient flowers), $Q(s)$. $N(s)$ corresponds to a solid line and the left scale, and $Q(s)$ corresponds to a dashed line and the right scale. Unlike the monotonic dependence of $N(s)$, $Q(s)$ is maximized at a certain stickiness allocation, s_Q . In this case, $s_Q = 0.186$. $R = 100000$, $\gamma_0 = 0.50$, $\rho_0 = 0.050$, $a = 5.0$, $b = 1.0$, $T = 1.0$, and $D = 0.10$.

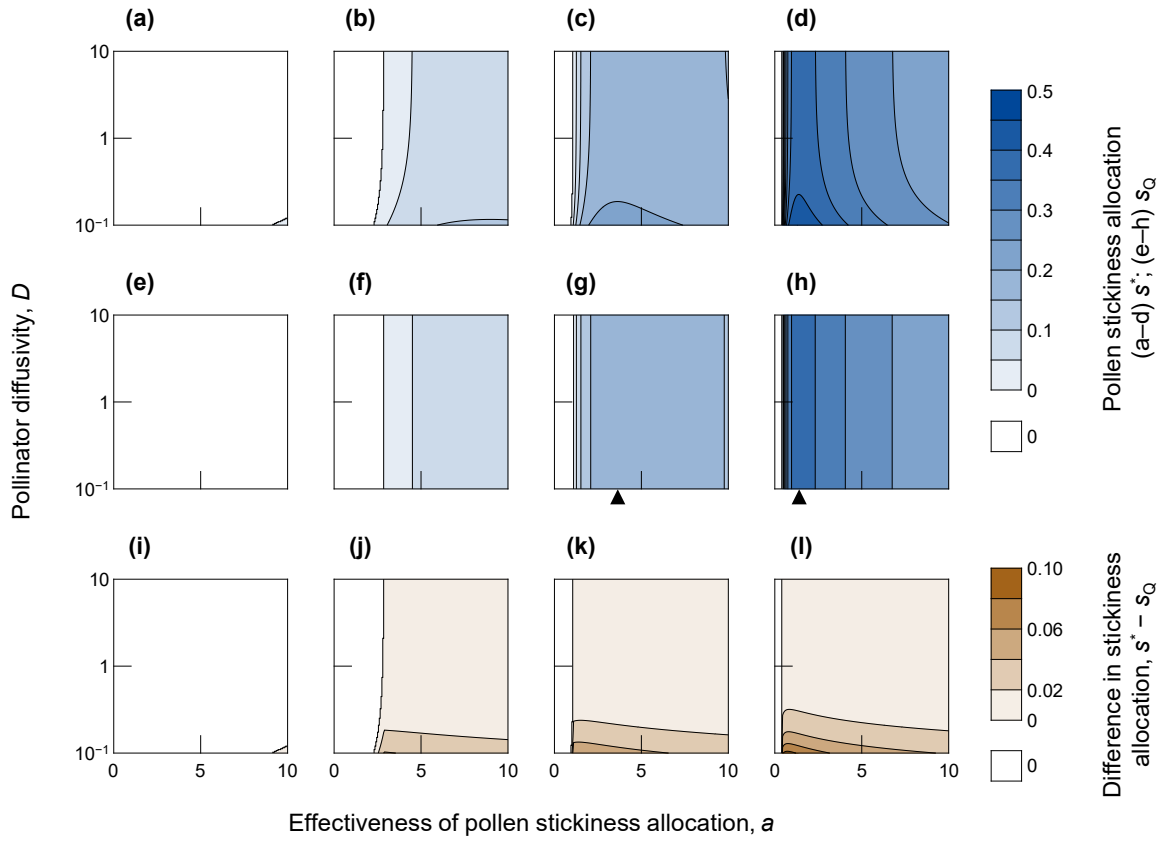


Fig. I-4. Dependences of (a–d) the evolutionarily stable pollen stickiness allocation, s^* , (e–h) the pollen stickiness allocation s_Q , which maximizes overall pollen deposition, $Q(s)$, and (i–l) the difference in these values, $s^* - s_Q$, on effectiveness of pollen stickiness allocation, a , and the pollinator diffusion coefficient, D . The maximum proportion of pollen loss from a pollinator body during a flight between two flowers, γ_0 , equals 0.10 (a, e and i), 0.30 (b, f and j), 0.50 (c, g and k) or 0.70 (d, h and l). The triangular arrow on the horizontal axis on each panel on the middle row indicates a that maximizes s_Q : $a = 67.5$ (e, out of the range), $a = 10.8$ (f, out of the range), $a = 3.82$ (g), and $a = 1.41$ (h). $R = 100000$, $b = 1.0$, $\rho_0 = 0.10$, and $T = 1.0$. The vertical axis on each panel is depicted on a logarithmic scale.

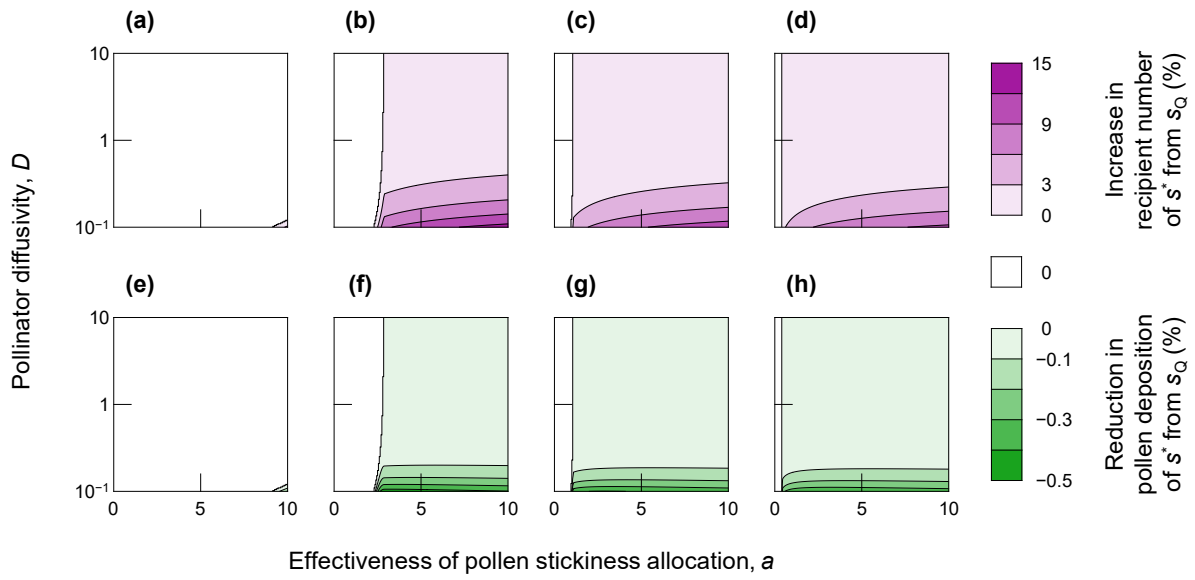


Fig. I-5. Dependences of (a–d) the percentage increase in the effective number of pollen recipient flowers, $N(s)$, of s^* compared with that of s_Q and (e–h) the percentage reduction in overall pollen deposition, $Q(s)$, on effectiveness of pollen stickiness allocation, a , and the pollinator diffusion coefficient, D . Here, s^* is the evolutionarily stable stickiness allocation, and s_Q is the stickiness allocation maximizing $Q(s)$. The maximum proportion of pollen loss from a pollinator body during a flight between two flowers, γ_0 , equals 0.10 (a and e), 0.30 (b and f), 0.50 (c and g) or 0.70 (d and h). $R = 100000$, $b = 1.0$, $\rho_0 = 0.10$, and $T = 1.0$. The vertical axis on each panel is depicted on a logarithmic scale.

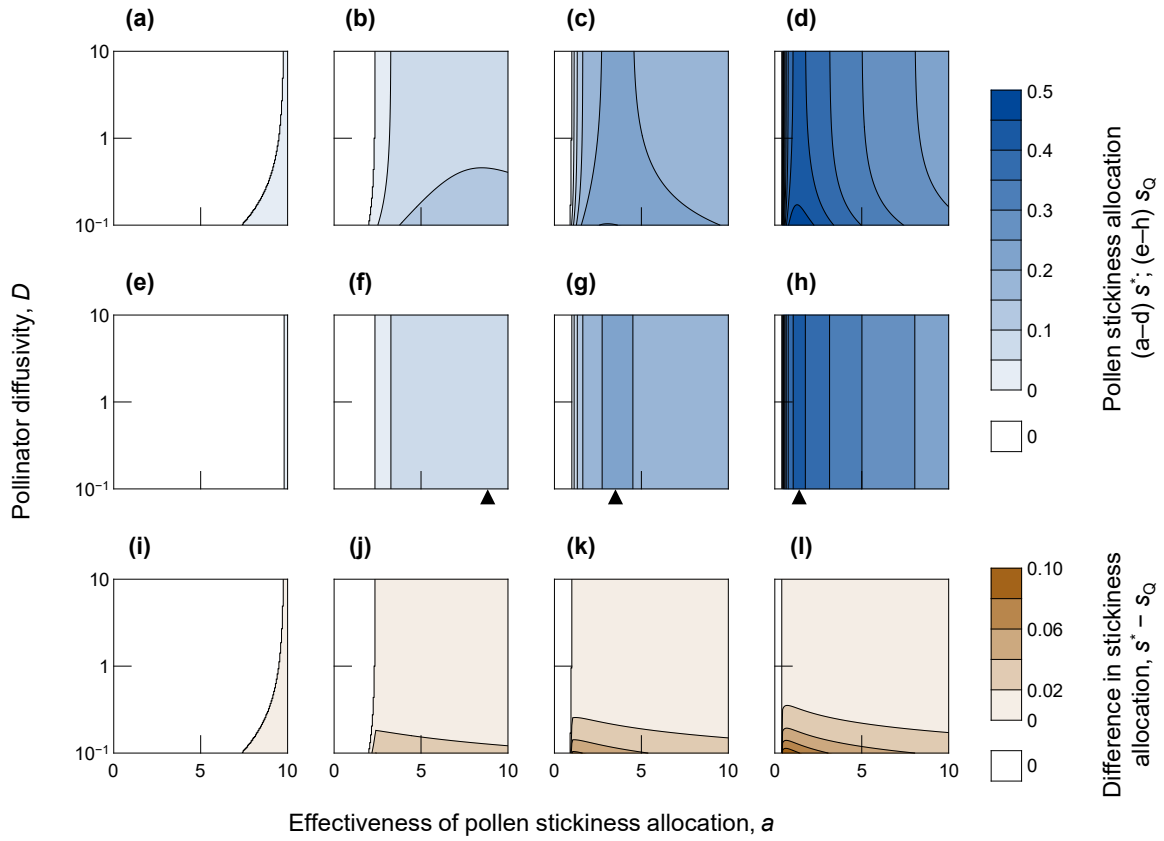


Fig. I-B1. Dependences of (a–d) the evolutionarily stable pollen stickiness allocation, s^* , (e–h) the pollen stickiness allocation s_Q , which maximizes overall pollen deposition, $Q(s)$, and (i–l) the difference in these values, $s^* - s_Q$, on effectiveness of pollen stickiness allocation, a , and the pollinator diffusion coefficient, D . The maximum proportion of pollen loss from a pollinator body during a flight between two flowers, γ_0 , equals 0.10 (a, e and i), 0.30 (b, f and j), 0.50 (c, g and k) or 0.70 (d, h and l). The triangular arrow on the horizontal axis on each panel on the middle row indicates a that maximizes s_Q : $a = 38.3$ (e, out of the range), $a = 8.79$ (f), $a = 3.46$ (g), and $a = 1.33$ (h). $R = 100000$, $b = 1.0$, $\rho_0 = 0.010$, and $T = 1.0$. The vertical axis on each panel is depicted on a logarithmic scale.

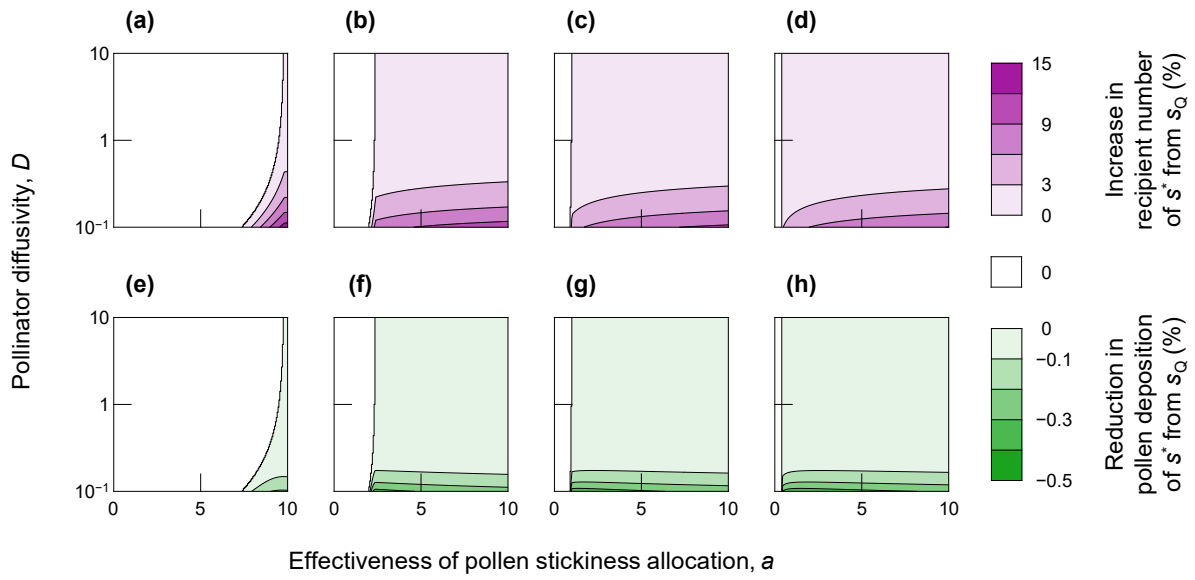


Fig. I-B2. Dependences of (a–d) the percentage increase in the effective number of pollen recipient flowers, $N(s)$, of s^* compared with that of s_Q and (e–h) the percentage reduction in overall pollen deposition, $Q(s)$, on effectiveness of pollen stickiness allocation, a , and the pollinator diffusion coefficient, D . Here, s^* is the evolutionarily stable stickiness allocation, and s_Q is the stickiness allocation maximizing $Q(s)$. The maximum proportion of pollen loss from a pollinator body during a flight between two flowers, γ_0 , equals 0.10 (a and e), 0.30 (b and f), 0.50 (c and g) or 0.70 (d and h). $R = 100000$, $b = 1.0$, $\rho_0 = 0.010$, and $T = 1.0$. The vertical axis on each panel is depicted on a logarithmic scale.

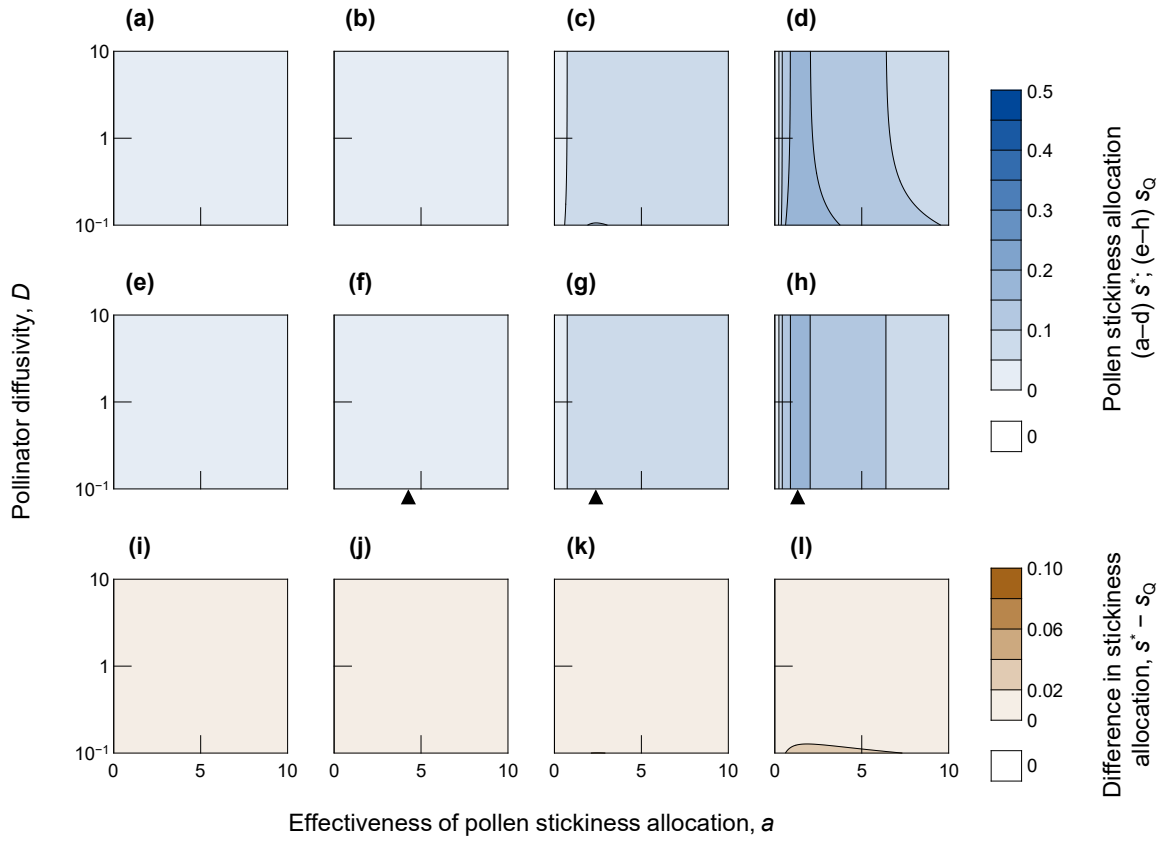


Fig. I-C1. Dependences of (a–d) the evolutionarily stable pollen stickiness allocation, s^* , (e–h) the pollen stickiness allocation s_Q , which maximizes overall pollen deposition, $Q(s)$, and (i–l) the difference in these values, $s^* - s_Q$, on effectiveness of pollen stickiness allocation, a , and the pollinator diffusion coefficient, D . The maximum proportion of pollen loss from a pollinator body during a flight between two flowers, γ_0 , equals 0.10 (a, e and i), 0.30 (b, f and j), 0.50 (c, g and k) or 0.70 (d, h and l). The triangular arrow on the horizontal axis on each panel on the middle row indicates a that maximizes s_Q : $a = 11.21$ (e, out of the range), $a = 4.24$ (f), $a = 2.37$ (g), and $a = 1.32$ (h). $R = 100000$, $b = 0.5$, $\rho_0 = 0.10$, and $T = 1.0$. The vertical axis on each panel is depicted on a logarithmic scale.

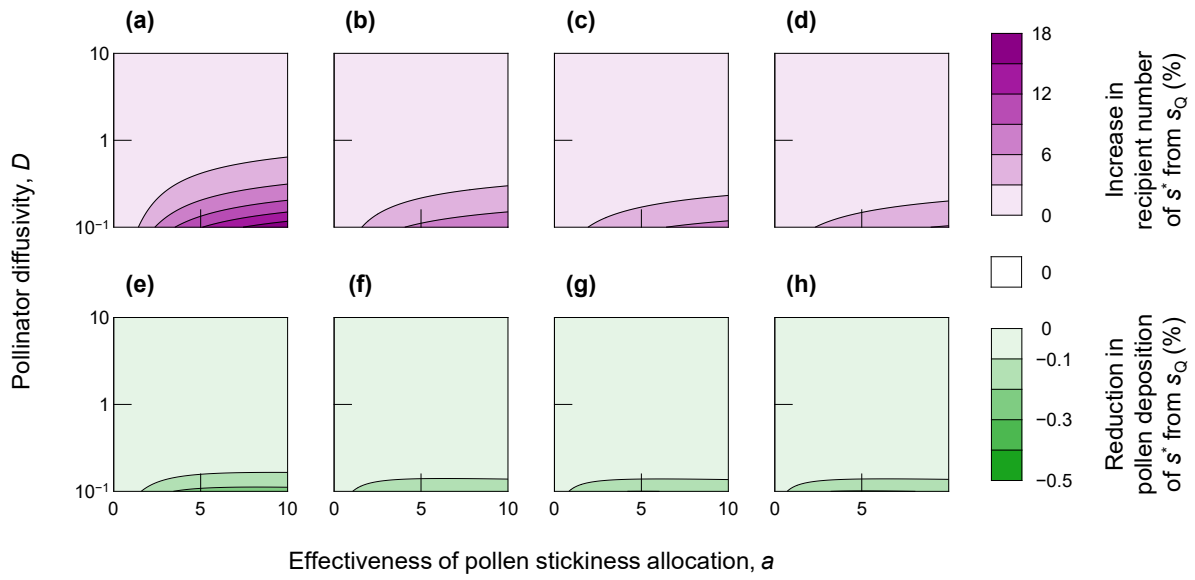


Fig. I-C2. Dependences of (a–d) the percentage increase in the effective number of pollen recipient flowers, $N(s)$, of s^* compared with that of s_Q and (e–h) the percentage reduction in overall pollen deposition, $Q(s)$, on effectiveness of pollen stickiness allocation, a , and the pollinator diffusion coefficient, D . Here, s^* is the evolutionarily stable stickiness allocation, and s_Q is the stickiness allocation maximizing $Q(s)$. The maximum proportion of pollen loss from a pollinator body during a flight between two flowers, γ_0 , equals 0.10 (a and e), 0.30 (b and f), 0.50 (c and g) or 0.70 (d and h). $R = 100000$, $b = 0.5$, $\rho_0 = 0.010$, and $T = 1.0$. The vertical axis on each panel is depicted on a logarithmic scale.

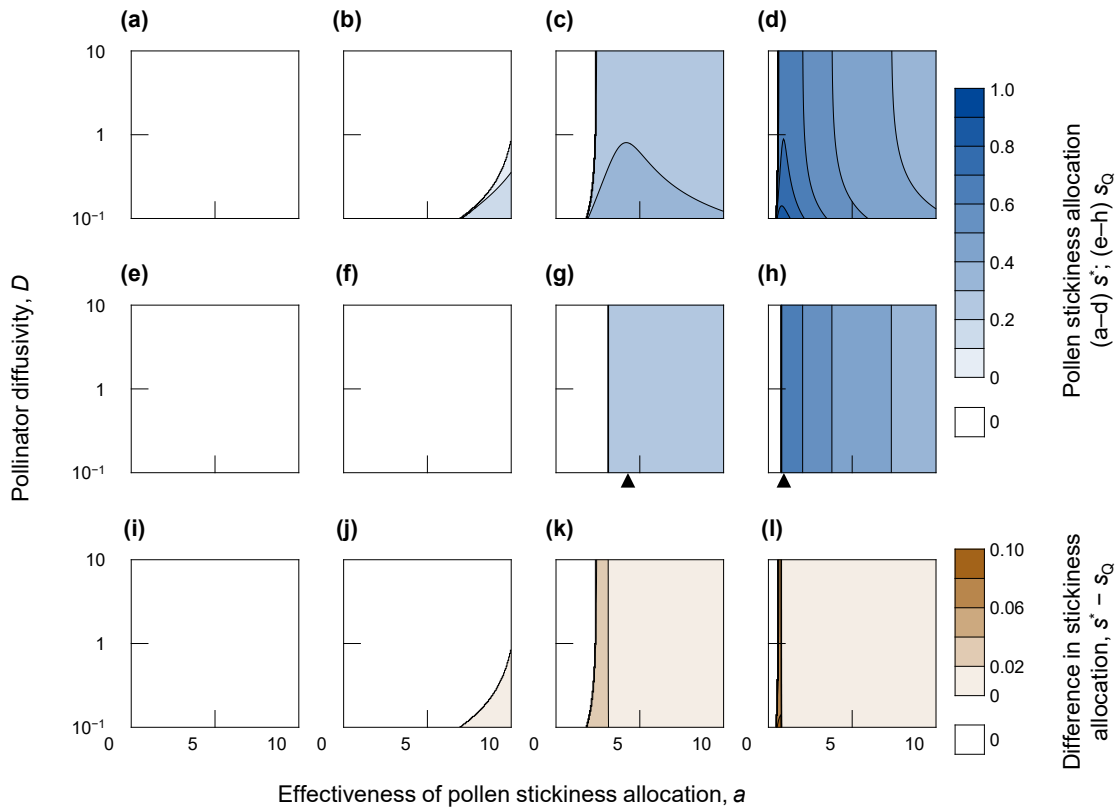


Fig. I-C3. Dependences of (a–d) the evolutionarily stable pollen stickiness allocation, s^* , (e–h) the pollen stickiness allocation s_Q , which maximizes overall pollen deposition, $Q(s)$, and (i–l) the difference in these values, $s^* - s_Q$, on effectiveness of pollen stickiness allocation, a , and the pollinator diffusion coefficient, D . The maximum proportion of pollen loss from a pollinator body during a flight between two flowers, γ_0 , equals 0.10 (a, e and i), 0.30 (b, f and j), 0.50 (c, g and k) or 0.70 (d, h and l). The triangular arrow on the horizontal axis on each panel on the middle row indicates a that maximizes s_Q : $a = 310.62$ (e, out of the range), $a = 20.23$ (f, out of the range), $a = 4.31$ (g), and $a = 0.92$ (h). $R = 100000$, $b = 1.5$, $\rho_0 = 0.10$, and $T = 1.0$. The vertical axis on each panel is depicted on a logarithmic scale. Note that panels in this figure have contours marked at intervals that are different from those in Figs. I-4, I-B1 and I-C1.

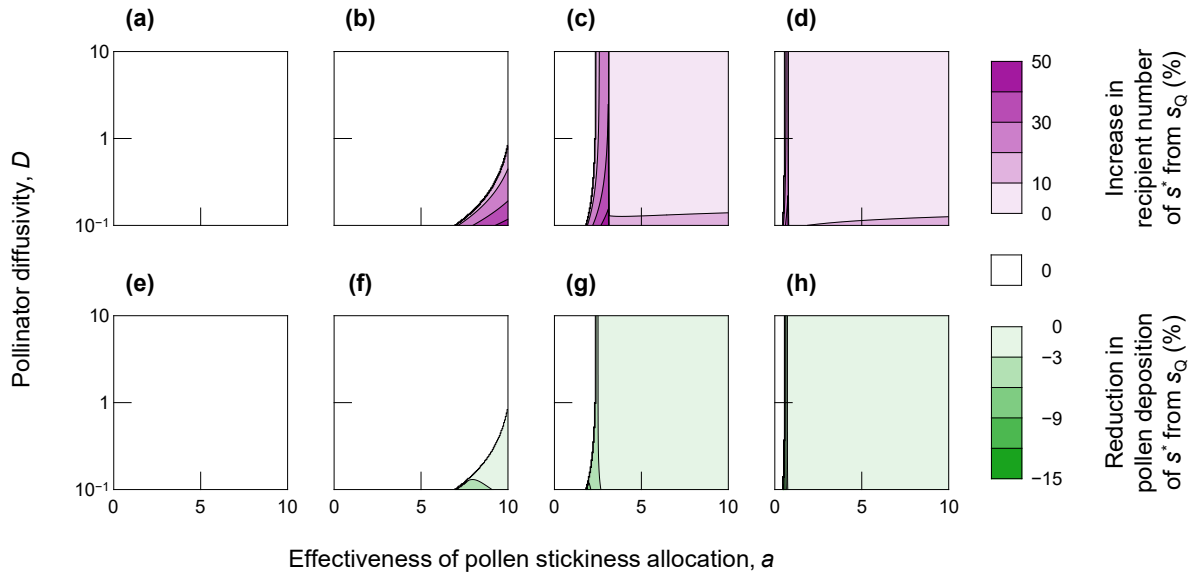


Fig. I-C4. Dependences of (a–d) the percentage increase in the effective number of pollen recipient flowers, $N(s)$, of s^* compared with that of s_Q and (e–h) the percentage reduction in overall pollen deposition, $Q(s)$, on effectiveness of pollen stickiness allocation, a , and the pollinator diffusion coefficient, D . Here, s^* is the evolutionarily stable stickiness allocation, and s_Q is the stickiness allocation maximizing $Q(s)$. The maximum proportion of pollen loss from a pollinator body during a flight between two flowers, γ_0 , equals 0.10 (a and e), 0.30 (b and f), 0.50 (c and g) or 0.70 (d and h). $R = 100000$, $b = 1.5$, $\rho_0 = 0.010$, and $T = 1.0$. The vertical axis on each panel is depicted on a logarithmic scale. Note that panels in this figure have contours marked at intervals that are different from those in Figs. I-5, I-B2 and I-C2.

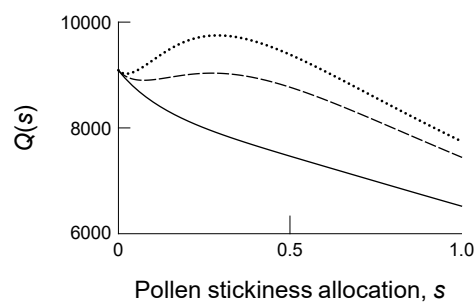


Fig. I-C5. The effects of pollen stickiness allocation on overall pollen deposition (the overall amount of pollen deposited on stigmas of the recipient flowers), $Q(s)$, if $b = 1.5$. $a = 1.0$ (a solid line), $a = 3.0$ (a dashed line), and $a = 5.0$ (a dotted line). $R = 100000$, $\gamma_0 = 0.50$, $\rho_0 = 0.10$.

Chapter II

Intraspecific variation in morphology of spiny pollen grains along an altitudinal gradient in an insect-pollinated shrub

Abstract

Intraspecific variations in pollen morphological traits are poorly studied. Interspecific variations are often associated with pollination systems and pollinator taxa. Altitudinal environmental changes, which can influence local pollinator assemblages, provide opportunities to explore differentiation in pollen traits of a single species over short distances. The aim of this study is to examine intraspecific variations in pollen traits of an insect-pollinated shrub, *Weigela hortensis* (Caprifoliaceae), along an altitudinal gradient. I compared pollen grain spine phenotypes (length, number and density), pollen grain diameter, lipid mass (pollenkitt) around pollen grains, pollen production per flower and pollinator assemblages at four sites at different altitudes. I found that spine length and the spine length/diameter ratio of pollen grains were greater at higher altitudes but not correlated with flower or plant size. Spine number and density increased as flower size increased, and lipid mass decreased as plant size increased. Bees were the predominant pollinators at low-altitude sites whereas flies, specifically hunch-back flies (*Oligoneura* spp., Acroceridae), increased in relative abundance with increasing altitude. These results suggest that the increase in spine length with altitude was the result of selection favoring longer spines at higher-altitude sites and/or shorter spines at lower-altitude sites. The altitudinal variation in selection pressure on spine length could reflect changes in local pollinator assemblages with altitude.

Introduction

Pollen grains are the carriers of male gametes in seed plants. They are morphologically different in many respects at various taxonomic levels despite having the same reproductive function

(Pacini and Franchi, 2020). Some of this variation has been attributed to pollen vectors that select for different sets of pollen traits. In general, compared to wind- and water-pollinated species, animal-pollinated species produce large pollen grains (Welsford et al., 2016), with elaborate exine structure (Tanaka et al., 2004) and are covered with a large amount of pollenkitt (Pacini and Hesse, 2005). Morphology of pollen grains is also diverse among plant species with different taxa of pollinators. Bat-pollinated species have larger pollen grains than their non-bat-pollinated relatives (Stroo, 2000). Echininate pollen is correlated with fly-pollinated species and psilate pollen with beetle-pollinated species in Araceae (Sannier et al., 2009). Within the genus *Erythrina* (Leguminosae), passerine-pollinated species produce pollen grains covered with more pollenkitt than hummingbird-pollinated species (Hemsley and Ferguson, 1985).

Although interspecific correlations between pollen traits and pollinator taxa have been well documented, to my knowledge, intraspecific correlations have never been reported. Considered together, several recent findings suggest that pollen traits may have differentiated within plant species according to differences in taxa of pollinators. In *Aconitum gymnantrum* (Ranunculaceae), which has a mixed insect- and wind-pollination system and produces two corresponding morphological types of pollen grains, the ratio of the two types differs between two populations that differ in the number of visiting bumble bees (Wang et al., 2017). In addition, quantitative traits of pollen grains that are likely to be picked up from a flower can vary among pollinator taxa. Pollen grains of *Taraxacum ceratophorum* (Asteraceae) picked up by bumble bees exhibit smaller variance of spine spacing and those picked up by flies exhibit larger diameters than expected at random (Lynn et al., 2020). This implies that bumble bees exert stabilizing selection on spine spacing of *T. ceratophorum* pollen grains while flies exert directional selection on the diameter of pollen grains. Moreover, as I theoretically demonstrated in Chapter I, the strength of selection favoring stickier pollen depends on pollinating partners that differ in morphology or behavior. Therefore, in a single plant species with various taxa of

pollinators, quantitative pollen traits such as size, spine phenotypes (e.g., length, number, and density) and amount of pollenkitt might differ between populations with different pollinators.

Taxa and abundance of pollinators of a plant species can differ among populations at different altitudes, reflecting distributions of animals and plants that are influenced by environmental changes with altitude (Lefebvre et al., 2018; McCabe and Cobb, 2021; Warren et al., 1988). Altitudinal environmental changes originate from a combination of general altitude phenomena such as the decline in air temperature and the reduction in land area with increasing altitude and local peculiarities such as precipitation, wind velocity and seasonality (Korner, 2007). Several studies addressed intraspecific altitudinal variations in floral traits that correlate with local pollinator assemblages. For example, in the spring-flowering shrub *Elaeagnus umbellata* (Elaeagnaceae) at three different altitudes in southwest China, the flowers of higher-altitude plants have longer corolla tubes and a higher volume of dilute nectar with a higher proportion of sucrose, which is associated with a change in the major pollinators from bees to sunbirds (Pi et al., 2021). Thus, altitudinal environmental changes, which can influence local pollinator assemblages, provide opportunities to explore adaptive differentiation in floral traits, including pollen traits, of a plant species over short distances (Byars et al., 2009; Korner, 2007; Nagano et al., 2014).

In this chapter, I examined altitudinal variations in quantitative pollen traits and flower visitor assemblages of the shrub *Weigela hortensis* (Caprifoliaceae). *Weigela hortensis* flowers produce echinate pollen grains covered with pollenkitt and are visited by flying insects from various taxa. I compared pollen grain spine phenotypes (length, number, and density), pollen grain diameter, amount of pollenkitt, pollen production per flower, and taxa and abundance of flower visitors at four sites at different altitudes. Pollen traits may vary depending on characteristics of local pollinators that may shift with altitude. This study is a first step toward identifying adaptive differentiation in pollen traits within a single plant species that is driven

by geographical differences in pollinator assemblages.

Material and Methods

Study species and sites

I studied pollen traits and flower visitor assemblages of *W. hortensis* (Caprifoliaceae) at four sites on Mt. Izumigatake, Miyagi, northern Honshu, Japan. *Weigela hortensis* is a deciduous shrub that occurs in mountainous areas in Japan. From May to June, it produces two or three pale rose, bell-shaped flowers in individual corymbs and corymbs form larger clusters with many flowers on individual branches (Fig. II-1a). The lifetime of an individual flower is typically 4–5 d (Suzuki and Ohashi, 2014). Corolla tubes are roughly 25–40 mm long. Pollen grains are echinate and covered with pollenkitt. Flowers are visited by various taxa of flying insects, including bees, flies, beetles and butterflies (Suzuki and Ohashi, 2014).

The four study sites lie at different altitudes on Mt. Izumigatake (Fig. II-2): Oizaka (38°22'30" N, 140°44'51" E, 277 m a.s.l.), Yoshinodaira (38°23'15" N, 140°43'00" E, 518 m a.s.l.), Otaira (38°24'51" N, 140°43'14" E, 650 m a.s.l.), and Taiwa (38°25'24" N, 140°42'35" E, 812 m a.s.l.). On Mt. Izumigatake *W. hortensis* commonly occurs on the roadside, and my highest-altitude study site (Taiwa) is located at the highest-altitude place that is accessible. The horizontal distance between any two of the four study sites is at least 1400 m. The altitudes given above are the benchmarks for each site. I studied individual plants growing approximately ± 10 m a.s.l. from the benchmark altitudes. *W. hortensis* blooms earliest at the lowest-altitude site, and progressively later at the higher-altitude sites.

Pollen sampling and trait measurements

From 28 May to 10 June 2020, I randomly selected ten *W. hortensis* plants with many mature buds and fresh flowers at each site. I sampled pollen from their buds or flowers to measure

pollen traits. I also measured the basal trunk diameter of each plant because it may correlate with pollen and/or floral traits.

To examine spine phenotypes and diameter of pollen grains, I collected pollen from five fresh flowers of each individual and dried it with silica gel for one month. For analysis with scanning electron microscopy, pollen was coated with platinum on an ion sputter coater (E-1045, Hitachi High-Tech, Japan) and observed using a scanning electron microscope (S-3400N, Hitachi High-Tech, Japan) at 3.0 kV. Six to ten (7.1 ± 0.6 , mean \pm s.d.) pollen grains from each flower were randomly selected and photographed. Then, the diameter, spine length and spine density of each pollen grain were measured using the images (Fig. II-3). The diameter of a pollen grain was defined as the diameter of the inscribed circle inside its outline detected mechanically using Mathematica 11.1 (Wolfram Research, 2017). The spine length was defined as the length of the longest spine forming a part of the outline of the grain. The spine density was calculated as the number of spines within the $500 \mu\text{m}^2$ circular area around the center of the grain. As small spines are unlikely to be involved in animal pollination, only spines with basal diameters over $1.0 \mu\text{m}$ were counted. In addition, the ratio of spine length to pollen grain diameter and the number of spines per grain were calculated. The number of spines per grain was estimated by multiplying spine density per unit area ($= \text{spine density}/500; \text{n} \cdot \mu\text{m}^{-2}$) by the pollen grain surface area ($= \pi \times \text{diameter}^2; \mu\text{m}^2$), assuming that the pollen grain is a perfect sphere. Spine length (μm), spine density ($\text{n} \cdot 500 \mu\text{m}^{-2}$), diameter (μm), spine length/diameter ratio and the number of spines per grain (n) were obtained for each of 1409 pollen grains and used for statistical analysis without including flower or individual mean (i.e., the unit of the analysis was a pollen grain). I also measured the corolla tube length of each flower because it may correlate with pollen traits (Sarkissian and Harder, 2001) or be subject to selection by pollinating partners (Anderson et al., 2014; Toji et al., 2021).

To examine pollen lipid mass, I collected anthers from 30–50 mature buds from each

plant and kept them at 30°C for a few days to induce anther dehiscence. As a result, sufficient pollen for lipid extraction was obtained from 38 of 40 plants and stored at -20°C prior to analysis. Approximately 5 mg pollen from each plant was placed on a polytetrafluoroethylene (PTFE) syringe-fitted filter (pore size 1.00 µm, Membrane Solutions, USA) and washed with a mixture of chloroform and methanol (3:1), a solvent for external lipids (Lin et al., 2013). Pollen was first washed with 5.0 ml of the mixture for 30 s and then washed briefly with 2.0 ml of the mixture three times. The filtrate was collected and dried at 25°C for 48 h. The lipid extracts obtained from the filtrates were weighed. Then, the pollen lipid mass (as the percentage of the total pollen mass) for each plant was calculated and used for statistical analysis.

To examine pollen production per flower, I collected all five anthers from each of five mature buds of each plant in 1.5 ml tubes containing 1.0 ml of 0.1% saline solution. Anthers were then dissected with a needle and placed in an ultrasonic cleaner for 1 min to release pollen grains. The pollen grains in 10 µl of saline solution were photographed under a dissecting microscope. All pollen grains in these images were counted using ImageJ (Schneider et al., 2012). Pollen production per flower (n), 1% of the total number of pollen grains contained in five anthers of a flower, was used for statistical analysis without including individual mean.

Flower visitor observation

To examine flower visitor assemblages of *W. hortensis* along an altitudinal gradient on Mt. Izumigatake, I conducted observations of flower visitors at the four sites for 8 days from 28 May to 10 June 2020 and for 11 days from 25 May to 11 June 2021. At least 15 individual plants with many fresh flowers were randomly selected and used for observations at each site in each year. During 90-min observation periods between 09:30 h and 12:00 h (in 2020 and 2021) or between 12:00 h and 14:30 h (in 2020), visitors to flowers on some branches of each plant were recorded with a digital video camera (HDR-CX420, HDR-CX680, Sony, Japan; GZ-R400, GZ-

RX690, JVCKENWOOD, Japan). From the video recordings, visits to 5–56 (17.4 ± 9.2 , mean \pm s.d.) flowers during each observation period were counted. Note that in this study, a single visit to a flower was defined as some part of an insect's body contacting an anther or a stigma during a bout of visiting the flower. Visitors were classified according to their taxa.

Statistical Analyses

All statistical models were developed in PyMC3, a probabilistic programming framework for Bayesian parameter estimation (Salvatier et al., 2016). Altitudinal variations in the following pollen traits were tested using hierarchical Bayesian models: spine length (μm), spine density ($n \cdot 500 \mu\text{m}^{-2}$), diameter (μm), spine length/diameter ratio, the number of spines per grain (n), pollen lipid mass (%) and pollen production per flower (n). All models included altitudes of sites where pollen was sampled as a predictor. The models for spine length, spine density, diameter, spine length/diameter ratio and the number of spines per grain included plant size (basal trunk diameter) and flower size (corolla tube length) as additional predictors. The models for lipid mass and pollen production included plant size as an additional predictor. All the models also included the two-way interactions of the predictors, and all predictors were standardized for improving the interpretation of the interaction effects and the efficiency of Markov chain Monte Carlo (MCMC) sampling. Sampling distributions and link functions appropriate for the outcome variables were used: gamma distributions and log link functions for spine length, diameter, spine length/diameter ratio, the number of spines per grain and lipid mass, Poisson distributions and log link functions for spine density and pollen production. The models for spine length, spine density, diameter, spine length/diameter ratio and the number of spines per grain included plant and flower (nested in plant) as random factors, that is, plant- and flower-specific random intercepts and a plant-specific random slope of flower size. If the random slope is omitted, observations from the same plant are treated as contributing

independent information about the moderating effect of plant size on the slope of flower size, resulting in severely anti-conservative statistical inference for the interaction between plant size and flower size and the main effect of flower size (Heisig and Schaeffer, 2019). Although plants were nested in one of the four sites at different altitudes, a site-specific random intercept or slope was omitted because at least five sites are required to achieve robust estimates of the variance among sites (Harrison, 2015; Harrison et al., 2018). The model for pollen production included a plant-specific random intercept.

Altitudinal variations in flower visitor assemblages were also tested using hierarchical Bayesian models with altitude as a predictor. Altitudinal variation in the number of visits per flower was analyzed with separate models according to visitor groups and time of observation (morning in 2020 or 2021 or afternoon in 2020). A negative binomial sampling distribution and a log link function were used with the total number of visits to flowers as an outcome variable and the number of flowers observed as an offset. In addition, altitudinal variations in the proportion of visits by individual visitor groups were analyzed with a logistic regression model using a binomial sampling distribution and a logit link function. Models for flower visitor assemblages included an observation-date-specific random intercept. Altitudinal variations in corolla tube length and basal trunk diameter were also tested. The model for corolla tube length included basal trunk diameter of individuals as an additional predictor and a plant-specific random intercept.

In all statistical analyses, the No-U-Turn Sampler was used to generate four MCMC chains each with 25,000 iterations following a burn-in period of 25,000 iterations. The potential scale reduction factors (R -hat) were below 1.01 for all parameters, indicating convergence of the MCMC chains. Variance inflation factors in the models with multiple predictors were at most 1.75, suggesting that there were no problems of multicollinearity (Dormann et al., 2013).

Results

Variations in pollen traits along an altitudinal gradient

Spine length of *W. hortensis* pollen grains was longer at higher altitudes (Fig. II-4a; Table II-1). The model-estimated median spine length of pollen grains produced by individuals at the highest-altitude site (Taiwa) was 19.9% larger than at the lowest-altitude site (Oizaka) (Figs. II-5 and II-6). Pollen grain diameter was not correlated with altitude, any other predictors, or their interactions (Fig. II-4b; Table II-1). Correspondingly, the spine length/diameter ratio was larger at higher altitudes (Fig. II-4c; Table II-1). Spine density was not correlated with altitude but was marginally and positively correlated with flower size (Fig. II-4d; Table II-1). The number of spines per grain, which is proportional to the product of spine density and diameter squared, was not correlated with altitude but increased with flower size (Fig. II-4e; Table II-1). Lipid mass was not correlated with altitude but decreased with plant size (Fig. II-4f; Table II-1). Pollen production per flower was not correlated with altitude, any other predictors, or their interactions (Fig. II-7a; Table II-1).

Flower size was influenced by both altitude and the interaction between altitude and plant size (Fig. II-7b; Table II-1). It was smaller at higher altitudes unless plant size was one standard deviation smaller than the average. Plant size was not correlated with altitude (Fig. II-7c; Table II-1).

Variations in flower visitor assemblages along an altitudinal gradient

The main visitors to flowers of *W. hortensis* were bumble bees (*Bombus* spp., Apidae), small bees, flies (Diptera), and beetles (Coleoptera) (Table II-2). Each of these taxa accounted for more than 10% of visiting insects at one or more study site(s). Small bees possibly included Andrenidae, Halictidae, Megachilidae, and Colletidae although their families were rarely identifiable on the video recordings. Hunch-back flies (*Oligoneura* spp., Acroceridae; Fig. II-

1b), which have large, rounded thoraxes and feed on flower nectar with their long proboscises, accounted for 83.3% of all visiting flies. I sometimes observed them mating inside flowers. Beetles seemed to be ineffective pollinators because they generally crawled over the mouth of the corolla tube, leading to some momentary contact of their legs with stigmas or anthers. Thus, subsequent analyses did not include beetles or butterflies and moths (Lepidoptera), which were rarely observed to visit flowers of *W. hortensis* (Table II-2).

Bumble bees visited flowers more frequently as altitude decreased in the morning in 2020 although altitudinal variation was not observed in the afternoon in 2020 or in the morning in 2021 (Table II-3). The number of visits by small bees was not significantly correlated with altitude in 2020 or 2021 (Table II-3). Flies visited flowers more frequently as altitude increased in both 2020 and 2021 (Table II-3). Consequently, the proportion of flies among the three visitor groups (bumble bees, small bees and flies) increased as altitude increased in both 2020 and 2021 (Fig. II-8; Table II-3). The model-estimated medians of the proportion of flies at the highest-altitude site (Taiwa) were 55.8% (in the morning in 2020), 67.9% (in the afternoon in 2020) and 20.6% (in the morning in 2021).

Discussion

Altitudinal variations in spine length of pollen grains and flower visitor assemblages

I found an altitudinal variation in a spine phenotype of echinate pollen grains of *W. hortensis*. Spine length of *W. hortensis* pollen grains was longer at higher-altitude sites (Fig. II-4a). The spine length/diameter ratio was also larger at higher altitudes (Fig. II-4c), suggesting that the increase in spine length with altitude was not the result of allometric scaling between spines and pollen grain size. In addition, spine length of pollen grains was not correlated with the size of flowers or plants that produced the pollen grains (Table II-1). Hence, spine length of pollen grains presumably did not depend on the reproductive resources of flowers and plants. These

results suggest that the increase in spine length with altitude was the result of selection favoring longer spines at higher-altitude sites and/or shorter spines at lower-altitude sites.

I also found altitudinal variation in assemblages of flower visitors of *W. hortensis*. Bees were the predominant visitors at low-altitude sites whereas flies, specifically hunch-back flies, increased in relative abundance with increasing altitude (Fig. II-8; Table II-2). This altitudinal gradient of pollinator assemblages from bees to flies is consistent with the general distribution pattern observed worldwide (Lefebvre et al., 2018; McCabe and Cobb, 2021; Warren et al., 1988).

These results raise the possibility that the spine phenotype of *W. hortensis* pollen grains has differentiated in response to altitudinal differences in assemblages of pollinators. The decrease in flower size with increasing altitude (Fig. II-7b) may also correspond to relatively small bodies of hunch-back flies, which increased in abundance with altitude (Fig. II-8). As with spine length, the decrease in flower size with altitude was probably not the result of a resource constraint because flower size was not correlated with plant size (Table II-1) and plant size was not correlated with altitude (Fig. II-7c; Table II-1).

Possible mechanisms of the differentiation in spine length of pollen grains

Spines of pollen grains probably mediate adhesion between pollen grains and pollinators. Theoretical work in Chapter I suggested that enhanced adhesion between pollen grains and pollinators contributes to parental reproductive success not only by diminishing pollen loss during transport but also by distributing pollen grains to a larger number of recipient flowers. Toward enhancing adhesion between pollen grains and pollinators, spine length of pollen grains could be subject to selection by morphological features of pollinators. Bees and hunch-back flies are obviously different in many morphological aspects; in particular, hair density is lower in hunch-back flies than bumble bees and small bees (personal observation). This is consistent

with the measurements of Roquer-Beni et al. (2020) showing that hair density is lowest in non-hoverfly flies, followed by beetles, hoverflies, bees, and butterflies and moths. The increase in spine length with altitude might be associated with low hair density of hunch-back flies, which increased in abundance with altitude. Pollen grains on sparse hair of pollinators contact only a few hairs and thus experience a small contact force whereas pollen grains on thick hair of pollinators contact more hairs and experience a larger force (Amador et al., 2017). When pollen grains are picked up by pollinators with low hair density such as hunch-back flies, longer spines of the pollen grains could increase the possibility of contact with more hairs and greater adhesion to them. In contrast, when pollen grains are picked up by pollinators with high hair density such as bees, spine length may have little effect on the degree of adhesion to the pollinators. Therefore, long spines of pollen grains could be selected for by pollinators with low hair density such as hunch-back flies. This hypothesis is consistent with my results that spine length was the longest at the highest-altitude site (Taiwa), where hunch-back flies were abundant.

Spine length of pollen grains could also influence pollen collecting behavior of bees. In the video recordings, I noticed that bees and hunch-back flies had different foraging behavior; bumble bees and small bees occasionally collected *W. hortensis* pollen on their corbiculae or scopae directly from the anthers or from their bodies by grooming while visiting hunch-back flies did not consume pollen but fed on nectar or mated inside flowers. Pollen grains collected on the corbiculae of bees are carried to the nest for larval provisioning and therefore do not contribute to plant reproductive success. Several studies demonstrated that long spines of pollen grains of some species interfere with active pollen collection on the corbiculae of bees (Konzmann et al., 2019; Lunau et al., 2015; Vaissière and Vinson, 1994). I can therefore hypothesize that long spines will be selected for by the pollen collecting behavior of bees. However, this hypothesis contradicts the results that spines of *W. hortensis* pollen grains were

relatively short in the lowest-altitude site (Oizaka), where bees were the predominant visitors. Bumble bees and small bees carried a large amount of *W. hortensis* pollen on their corbiculae and scopae not only at the lowest-altitude site (Oizaka), where spines were short, but also at the highest-altitude site (Taiwa), where spines were long (personal observation). This implies that the presence and the length of spines of *W. hortensis* pollen grains did not interfere with pollen collection on pollen transport structures by bumble bees and small bees.

In summary, the increase in spine length with altitude may be the result of selection exerted by the low hair density of hunch-back flies that favors long spines at higher-altitude sites. Further work is required to identify what characteristics of pollinators, or perhaps other factors, cause altitudinal variation in spine length of *W. hortensis* pollen grains.

Pollen traits independent of altitude

In contrast to spine length, spine density and the number of spines per grain were not correlated with altitude. They increased as flower size increased (Table II-1). Spine density and number could play important roles in adhesion to insects and interference with pollen collection by bees. Bees and flies, which differ in relative abundance depending on altitude, may exert similar selection or may not exert strong selection on spine density and spine number of *W. hortensis* pollen grains. On the other hand, adding spines may require additional resources. In that case, larger flowers, which may have more resources, could afford more spines on pollen grains although further work is required to determine whether added spines increase pollination success of pollen grains or not.

Pollen grain diameter was also not correlated with altitude (Fig.II-4b; Table II-1). Pollen grain size may be influenced by multiple factors such as pollinators (Amador et al., 2017; Hao et al., 2020; Konzmann et al., 2019), temperature (Ejsmond et al., 2015) and soil nitrogen (Lau and Stephenson, 1993), which generally vary with altitude (Korner, 2007; Lefebvre et al., 2018;

McCabe and Cobb, 2021; Tashi et al., 2016). Therefore, even if one of the factors imposes selection or a constraint such that pollen grain size increases or decreases with altitude, another factor could offset the effect by imposing the opposite selection or constraint, resulting in small altitudinal variation in pollen grain size. Additionally, during post-pollination processes, large pollen grains may outperform small ones in pollen competition for ovule fertilization (McCallum and Chang, 2016). If a minimum pollen grain size is required for fertilizing an ovule and above this minimum an increase in pollen grain size leads to diminishing returns in the probability of fertilization, there would be an optimal pollen grain size maximizing parental reproductive success in post-pollination processes with limited reproductive resources (Smith and Fretwell, 1974; Vonhof and Harder, 1995). This may explain why diameters of *W. hortensis* pollen grains were also independent of flower and plant size (Table II-1).

Pollen lipid mass was also not correlated with altitude but decreased as plant size increased (Fig.II-4f; Table II-1). In addition, lipid mass of *W. hortensis* pollen ($8.1 \pm 1.8\%$, mean \pm s.d., $n = 38$) is much smaller than that of echinate pollen grains of *Taraxacum officinale* (Asteraceae; mean = 60%) or *Helianthus annuus* (Asteraceae; mean = 30%) reported by Lin et al. (2013). In general, pollenkit covering pollen grains has a variety of functions. Some are related to pollinators (e.g., attracting pollinators, facilitating adhesion to pollinators, and providing a digestible reward for pollinators), and some are related to other biotic and abiotic factors (e.g., avoiding predation of pollen grains, keeping pollen grains together during transport, and protecting pollen grains from water loss and UV radiation) (Pacini and Hesse, 2005). Therefore, even if pollen lipid mass is partly subject to selection by the altitudinal variation in pollinator assemblages, that selection could be masked by stabilizing selection by other factors. Further work, including quantifying pollen lipid mass for individual flowers, is required to explain what factors impose selection on lipid mass of *W. hortensis* pollen and why lipid mass was small in pollen of large plants.

Conclusions

I found altitudinal variation in spine length of *W. hortensis* pollen grains; spines were longer at higher altitudes (Fig.II-4a). The spine length/pollen grain diameter ratio was also larger at higher altitudes (Fig.II-4c), suggesting that the increase in spine length with altitude was not the result of allometric scaling between spines and pollen grain size but the result of selection acting directly on spine length. I also found that bees were the predominant flower visitors in low-altitude sites whereas flies, specifically hunch-back flies, increased in relative abundance with increasing altitude (Fig. II-8). This study encourages further research to identify adaptive differentiation in pollen traits within a plant species that is driven by geographical differences in pollinator assemblages.

Table II-1. Posterior coefficient estimates from hierarchical Bayesian models for pollen traits, flower size (corolla tube length) and plant size (basal trunk diameter). (a–h) Multiple regression analyses and (i) a simple regression analysis were conducted. All estimated coefficients are listed as the median with the 95% highest density interval (HDI) in parentheses.

	Posterior median	(95% HDI)
(a) Spine length		
Altitude	0.066	(0.023, 0.111)
Plant size	0.006	(−0.035, 0.045)
Flower size	0.014	(−0.015, 0.043)
Altitude × Plant size	0.015	(−0.030, 0.058)
Altitude × Flower size	−0.009	(−0.037, 0.020)
Plant size × Flower size	−0.004	(−0.033, 0.025)
(b) Diameter		
Altitude	−0.008	(−0.025, 0.008)
Plant size	0.002	(−0.014, 0.017)
Flower size	0.005	(−0.003, 0.013)
Altitude × Plant size	−0.002	(−0.018, 0.015)
Altitude × Flower size	0.002	(−0.006, 0.010)
Plant size × Flower size	0.001	(−0.007, 0.010)
(c) Spine length/diameter ratio		
Altitude	0.076	(0.031, 0.122)
Plant size	0.007	(−0.035, 0.048)
Flower size	0.009	(−0.021, 0.039)
Altitude × Plant size	0.018	(−0.027, 0.062)
Altitude × Flower size	−0.009	(−0.038, 0.021)
Plant size × Flower size	−0.005	(−0.035, 0.026)

Table II-1. (continued)

	Posterior median	(95% HDI)
(d) Spine density		
Altitude	-0.011	(-0.083, 0.058)
Plant size	0.014	(-0.052, 0.079)
Flower size	0.039	(-0.001, 0.079)
Altitude × Plant size	0.062	(-0.011, 0.137)
Altitude × Flower size	0.020	(-0.020, 0.058)
Plant size × Flower size	0.012	(-0.029, 0.053)
(e) The number of spines per grain		
Altitude	-0.028	(-0.100, 0.044)
Plant size	0.018	(-0.047, 0.084)
Flower size	0.048	(0.006, 0.091)
Altitude × Plant size	0.063	(-0.013, 0.140)
Altitude × Flower size	0.025	(-0.017, 0.066)
Plant size × Flower size	0.017	(-0.026, 0.061)
(f) Pollen lipid mass		
Altitude	-0.034	(-0.108, 0.041)
Plant size	-0.111	(-0.181, -0.043)
Altitude × Plant size	0.003	(-0.076, 0.078)
(g) Pollen production		
Altitude	-0.008	(-0.077, 0.063)
Plant size	-0.033	(-0.097, 0.032)
Altitude × Plant size	-0.024	(-0.095, 0.048)
(h) Flower size		
Altitude	-0.049	(-0.081, -0.017)
Plant size	-0.021	(-0.050, 0.008)
Altitude × Plant size	-0.048	(-0.080, -0.015)
(i) Plant size		
Altitude	0.083	(-0.027, 0.198)

Table II-2. The number of insect visits per flower during a 90-min observation period at the four study sites. Means \pm s.d. (in parentheses) are shown. Flower visitor observations were conducted in the morning (90-min periods between 09:30 h and 12:00 h) in 2020 and 2021 and in the afternoon (90-min periods between 12:00 h and 14:30 h) in 2020. Small bees possibly included Andrenidae, Halictidae, Megachilidae, and Colletidae. Honey bees (*Apis*, Apidae), carpenter bees (*Xylocopa*, Apidae) and wasps were also observed with very low frequency.

Morning in 2020				
Visitor group	The number of visits per flower			
	Oizaka	Yoshinodaira	Otaira	Taiwa
Hymenoptera				
Bumble bees	0.11 (0.03)	0.04 (0.01)	0	0
Small bees	0.86 (0.09)	0.91 (0.08)	1.15 (0.09)	0.81 (0.09)
Diptera				
Hunch-back flies	0.01 (0.01)	0.01 (0.01)	0.10 (0.03)	1.56 (0.22)
Hoverflies	0.04 (0.02)	0.02 (0.01)	0.03 (0.01)	0.02 (0.01)
Unidentified flies	0	0.09 (0.02)	0.04 (0.01)	0.05 (0.02)
Coleoptera	0.08 (0.03)	0.00 (0.00)	0.31 (0.05)	0.35 (0.05)
Lepidoptera	0.04 (0.01)	0.03 (0.01)	0.01 (0.01)	0
Afternoon in 2020				
Hymenoptera				
Bumble bees	0.10 (0.03)	0.03 (0.01)	0.03 (0.01)	0
Small bees	0.53 (0.07)	0.7 (0.06)	0.8 (0.07)	0.63 (0.09)
Diptera				
Hunch-back flies	0.01 (0.01)	0.02 (0.01)	0.14 (0.03)	1.70 (0.21)
Hoverflies	0.02 (0.01)	0.04 (0.01)	0.00 (0.00)	0.01 (0.01)
Unidentified flies	0.02 (0.01)	0.14 (0.04)	0.05 (0.02)	0.01 (0.01)
Coleoptera	0.17 (0.05)	0	0.3 (0.05)	0.29 (0.06)
Lepidoptera	0.02 (0.01)	0	0.03 (0.01)	0.03 (0.01)

Table II-2. (continued)

Morning in 2021				
Visitor group	The number of visits per flower			
	Oizaka	Yoshinodaira	Otaira	Taiwa
Hymenoptera				
Bumble bees	0.06 (0.01)	0.03 (0.01)	0.13 (0.02)	0.09 (0.01)
Small bees	0.59 (0.05)	0.91 (0.06)	0.55 (0.05)	1.02 (0.06)
Diptera				
Hunch-back flies	0.00 (0.00)	0.00 (0.00)	0.11 (0.03)	0.53 (0.08)
Hoverflies	0.04 (0.01)	0	0.02 (0.01)	0.04 (0.01)
Unidentified flies	0.01 (0.00)	0.03 (0.01)	0.03 (0.01)	0.03 (0.01)
Coleoptera	0.06 (0.02)	0.08 (0.02)	0.15 (0.03)	0.20 (0.02)
Lepidoptera	0.03 (0.01)	0.00 (0.00)	0.00 (0.00)	0.02 (0.01)

Table II-3. Posterior coefficient estimates from hierarchical Bayesian models examining the effect of altitude on the number of insect visits per flower during a 90-min observation period and the proportion of flies among the three visitor groups (bumble bees, small bees and flies). All estimated coefficients are listed as the median with the 95% highest density interval (HDI) in parentheses.

	Posterior median	(95% HDI)
(a) Bumble bees		
Morning in 2020	-2.853	(-7.041, -0.108)
Afternoon in 2020	-1.545	(-4.314, 0.624)
Morning in 2021	0.256	(-0.465, 0.934)
(b) Small bees		
Morning in 2020	0.154	(-0.188, 0.539)
Afternoon in 2020	0.160	(-0.241, 0.592)
Morning in 2021	0.336	(-0.099, 0.773)
(c) Flies		
Morning in 2020	1.370	(0.746, 2.003)
Afternoon in 2020	1.419	(0.807, 2.043)
Morning in 2021	0.815	(0.140, 1.384)
(d) Proportion of flies		
Morning in 2020	1.525	(1.088, 1.973)
Afternoon in 2020	1.609	(1.178, 2.046)
Morning in 2021	0.508	(0.035, 0.948)

(a)



(b)



Fig. II-1. (a) A *Weigela hortensis* individual with many flowering branches. (b) A hunch-back fly (*Oligoneura* sp.) accumulating *W. hortensis* pollen on the dorsal hairs.

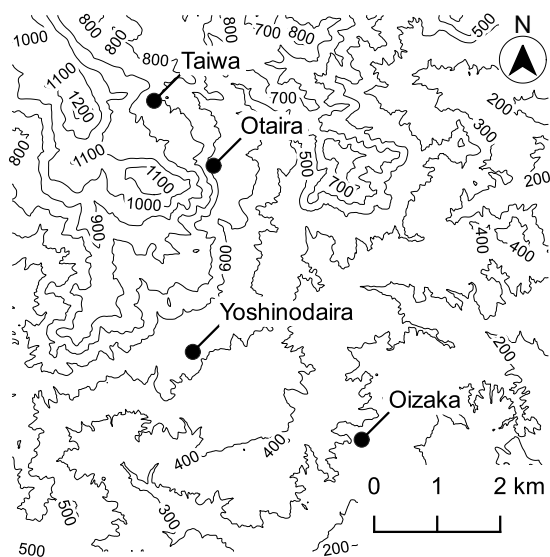


Fig. II-2. Locations of the four study sites on Mt. Izumigatake. Created from the Digital Elevation Model published by the Geospatial Information Authority of Japan.

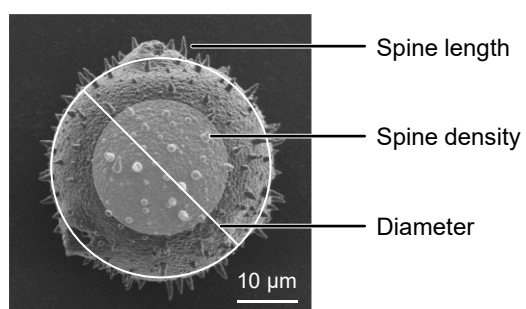


Fig. II-3. A scanning electron micrograph of a *W. hortensis* pollen grain (at 1000×) and trait measurements.

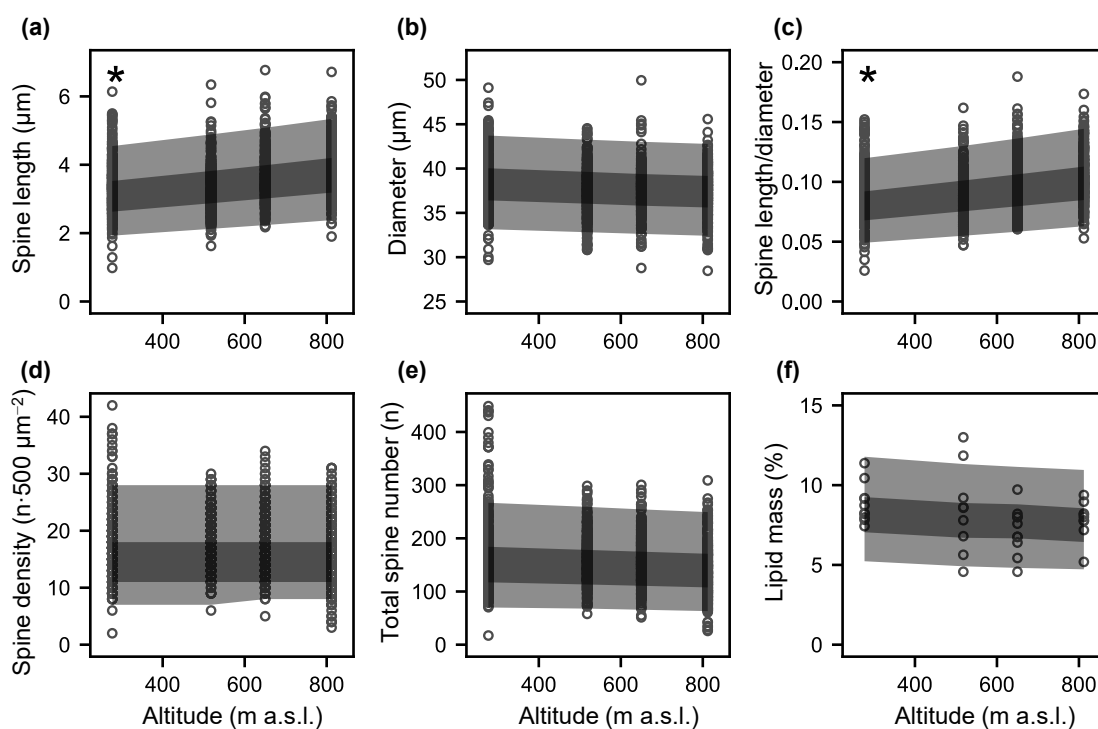


Fig. II-4. Altitudinal variations in (a) spine length, (b) diameter, (c) spine length/ diameter ratio, (d) spine density, (e) the number of spines per grain and (f) pollen lipid mass. Each data point represents the trait value of (a–e) a pollen grain or (f) a plant. The 50% (gray) and 95% (light gray) highest density intervals (HDI) of outcome variables were derived from hierarchical Bayesian models that hold the other predictors constant at their mean values and may include random factors. An asterisk in the upper left corner of a panel indicates that the 95% HDI of the coefficient of altitude did not include zero.

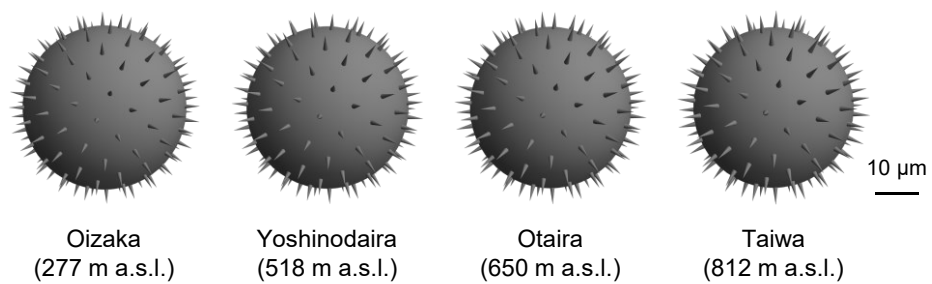


Fig. II-5. Images of *W. hortensis* pollen grains in the four study sites. These were created from the model-estimated medians of spine length (3.15, 3.41, 3.57 and 3.77 μm , from the lowest to the highest altitude), diameter (38.3, 37.9, 37.7 and 37.5 μm) and the number of spines per grain (159, 153, 151 and 147).

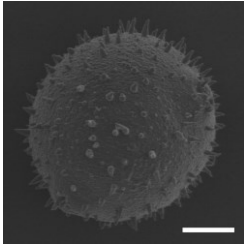
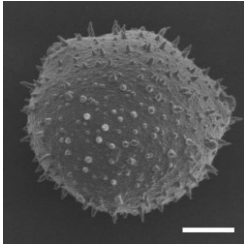
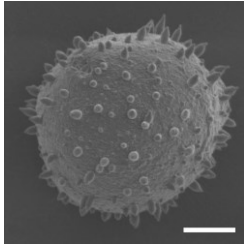
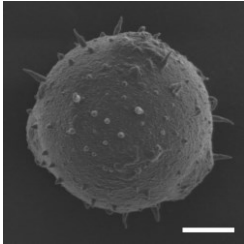
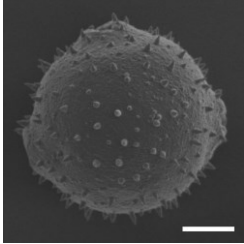
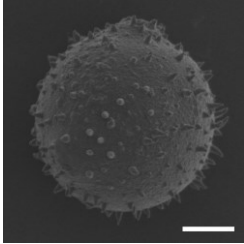
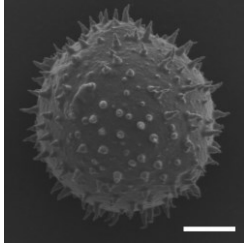
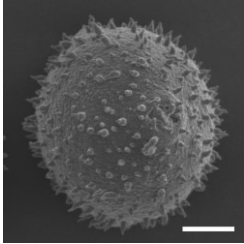
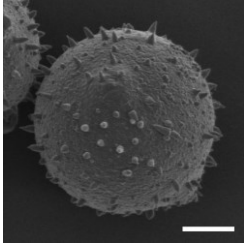
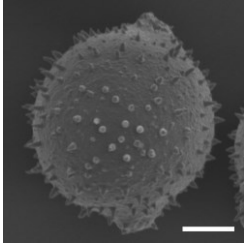
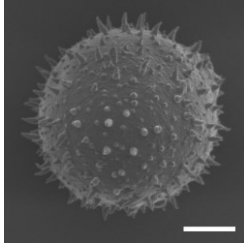
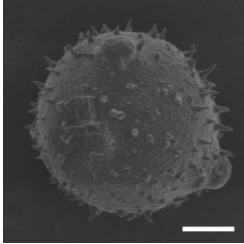
Rank	Oizaka	Yoshinodaira	Otaira	Taiwa
1st	 sl = 3.18, d = 38.1	 sl = 3.38, d = 38.0	 sl = 3.63, d = 37.7	 sl = 3.78, d = 37.3
2nd	 sl = 3.08, d = 38.6	 sl = 3.38, d = 38.1	 sl = 3.62, d = 37.9	 sl = 3.72, d = 37.6
3rd	 sl = 3.26, d = 38.4	 sl = 3.48, d = 38.2	 sl = 3.50, d = 37.7	 sl = 3.86, d = 37.6

Fig. II-6. Scanning electron micrographs (at 1000 \times) of *Weigela hortensis* pollen grains with spine lengths and diameters close to the model-estimated medians. For each of the four study sites, the top three pollen grains were selected using the following steps: (i) subtract the model-estimated medians from the trait values of an individual pollen grain, (ii) scale the differences by dividing them by the standard deviations, (iii) calculate the sum of squares of the scaled differences, and (iv) select the three pollen grains with the smallest sums of squares. The model-estimated medians are 3.15, 3.41, 3.57 and 3.77 μm for spine length, and 38.3, 37.9, 37.7 and 37.5 μm for diameter (from the lowest- to the highest-altitude site). sl: spine length (μm), d: diameter (μm). Scale bars: 10 μm .

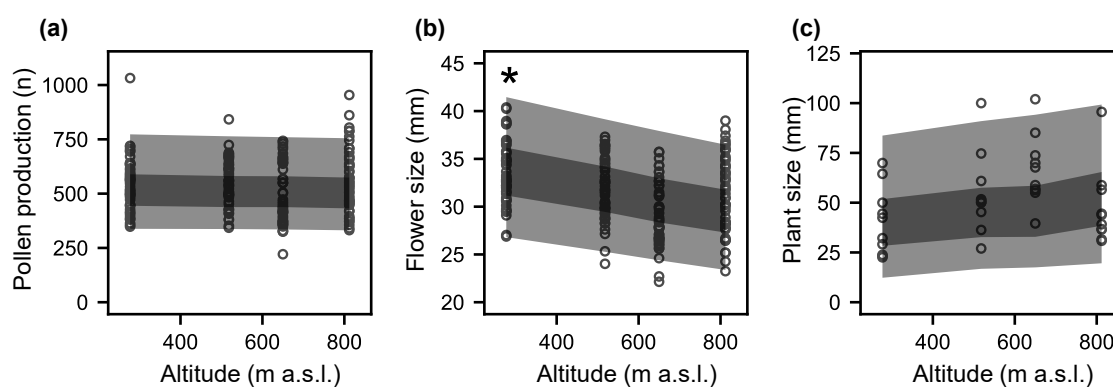


Fig. II-7. Altitudinal variations in (a) pollen production per flower, (b) flower size (corolla tube length) and (c) plant size (basal trunk diameter). Each data point represents the trait value of (a, b) a flower or (c) a plant. The 50% (gray) and 95% (light gray) highest density intervals (HDIs) of outcome variables were derived from hierarchical Bayesian models that hold the other predictors constant at their mean values and may include random factors. An asterisk in the upper left corner of a panel indicates that the 95% HDI of the coefficient of altitude did not include zero.

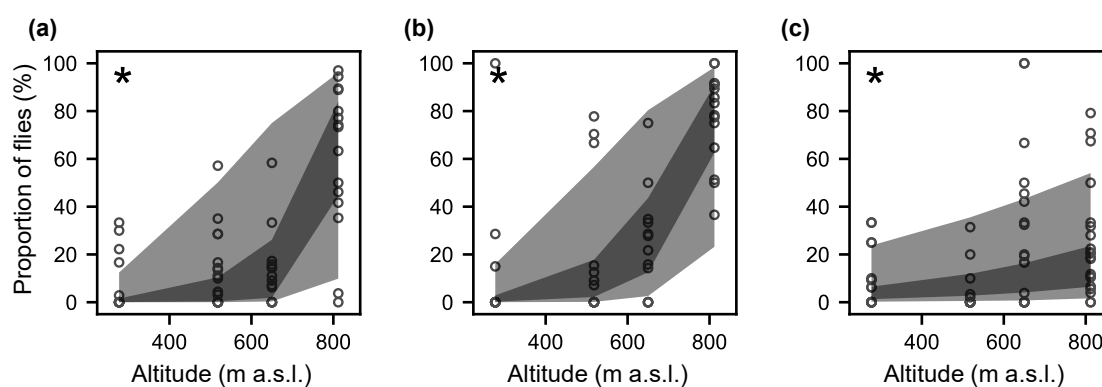


Fig. II-8. Altitudinal variations in the proportion of flies among the three pollinator functional groups (bumble bees, small bees and flies) (a) in the morning in 2020, (b) in the afternoon in 2020 and (c) in the morning in 2021. Each data point represents the observation outcome for an individual plant. The 50% (gray) and 95% (light gray) highest density intervals (HDIs) of the proportions were derived from hierarchical Bayesian models including observation date as a random factor. An asterisk in the upper left corner of a panel indicates that the 95% HDI of the coefficient of altitude did not include zero.

Chapter III

Pollen morphology for successful pollination dependent on pollinator taxa in a generalist plant: Relationship with foraging behavior

Abstract

Pollen morphology varies at inter- and intraspecific levels. Its interaction with pollinator behavior and morphology determines pollen fate. I tested whether pollen morphology promoting successful pollination differs depending on pollinator taxa in a generalist shrub, *Weigela hortensis* (Caprifoliaceae). I identified flower visitors carrying pollen from anthers to stigmas and compared the spine length and diameter of the pollen grains they carried. I found that pollen on the bodies of bumble bees and hunch-back flies and the scopae of small bees (including andrenid bees) contributed to seed production. Pollen grains on the bodies of bumble bees had longer spines than those on the scopae of andrenid bees or the bodies of hunch-back flies. Pollen grains on the scopae of andrenid bees had larger diameters than those on hunch-back flies. Bumble bees collected pollen grains with shorter spines and larger diameters on their corbiculae while andrenid bees collected pollen grains with shorter spines and intermediate diameters on their scopae. The differences in morphology of pollen carried by pollinators reflected pollen collection from bodies to corbiculae/scopae by bees. These findings suggest that pollen morphology has diversified to facilitate successful pollination by pollinating partners.

Introduction

Pollen grains are the carriers of male gametes that travel from anthers to stigmas in seed plants. In angiosperms, 87.5% of species rely on animals for pollination (Ollerton et al., 2011). Since there are multiple routes of pollen loss, such as pollen grooming and passive pollen loss during

transport (Inouye et al., 1994; Minnaar et al., 2019), only a small fraction of pollen in anthers reaches stigmas (Harder and Thomson, 1989; Rademaker et al., 1997). Thus, plant male reproductive success depends highly on pollen fate. As pollinating animals vary in behavior and morphology (Krauss et al., 2017; Roquer-Beni et al., 2020; Stavert et al., 2016; Thorp, 2000), flowers have evolved to facilitate pollen transfer from anthers to stigmas via their pollinating partners (e.g., Anderson et al., 2014; Castellanos et al., 2006; Parker et al., 2018).

Pollen morphology is diverse at various taxonomic levels and often considered responsible for the success of animal pollination in the context of pollinator behavior and morphology. In its interaction with pollinator behavior, pollen morphology may affect the probability of pollen collection from bodies to transport structures by bees, a major route of pollen loss in bee pollination (Holmquist et al., 2012; Minnaar et al., 2019; Thomson, 1986). A few studies comparing pollen collectability by bees among multiple plant species suggest that pollen grains with long spines or large diameters are less likely to be collected from bodies to pollen transport structures (Hao et al., 2020; Vaissière and Vinson, 1994). In the interaction between pollen and pollinator morphology, pollen spines could influence the probability of anchoring pollen grains to pollinator hairs (Lynn et al., 2020) while pollen grain size could influence the surface area contacting the hairs and therefore the contact force (Amador et al., 2017). Since insect hairs can vary in length and density among taxa (Roquer-Beni et al., 2020; Stavert et al., 2016), the spine length or size of pollen grains that adhere well to pollinators could depend on insect taxa. Lynn et al. (2020) examined the effects of intraspecific variation in pollen morphology on pollen pickup from flowers by bumble bees and flies in *Taraxacum ceratophorum* (Asteraceae). They found that pollen grains picked up by flies were larger in diameter (but not in spine length or spacing) than those picked up by bumble bees.

Thus, the fates of pollen grains depend largely on interactions of their morphology with pollinator foraging behavior and morphology. This suggests that pollen morphology facilitating

successful pollination could differ according to pollinator taxa. An opportunity to test this hypothesis is provided by quantitative variations in pollen morphology within a plant species with various pollinator taxa (i.e., a generalist plant species) although such intraspecific variations are largely unrecognized. To test the hypothesis, it is necessary to (1) identify flower visitors carrying pollen from anthers to stigmas and characterize their foraging behavior and then (2) compare quantitative morphological traits of the pollen grains carried by these pollinators.

In this chapter, I tested whether pollen morphology promoting successful pollination depends on pollinator taxa in the generalist shrub *Weigela hortensis* (Caprifoliaceae). In Chapter II, I showed that there were intraspecific variations in morphology of spiny pollen grains of *W. hortensis*, and the flowers were visited by various taxa of bees and flies that differed in foraging behavior. I identified flower visitors contributing to seed production as well as whether pollen on the transport structures of bees had a chance of stigma deposition and ovule fertilization. I also estimated the proportion of pollen carried by flower visitors that originated from *W. hortensis* flowers, which represents the degree of their fidelity to *W. hortensis* flowers and partly explains their pollination effectiveness. I then compared the spine lengths and diameters of *W. hortensis* pollen grains between the pollinator groups and examined the effects of these pollen traits on the probability that pollen was collected from bodies to pollen transport structures of pollinating bees. Based on these results, I discuss the impact of pollen morphology on success in the generalized pollination system of *W. hortensis*.

Material and Methods

Study species and sites

Weigela hortensis (Caprifoliaceae) is a deciduous shrub that occurs in mountainous areas in Japan. From May to June, it produces many pale rose, bell-shaped flowers with 25–40 mm-

long corolla tubes. Flowers are self-incompatible and typically last for 4–5 days (Suzuki and Ohashi, 2014). My preliminary survey showed that the number of ovules per flower was 69 ± 13 (mean \pm s.d., $n = 39$).

The three study sites lie at different altitudes on Mt. Izumigatake, northern Honshu, Japan: Yoshinodaira (38°23'15" N, 140°43'00" E, 518 m a.s.l.), Otaira (38°24'51" N, 140°43'14" E, 650 m a.s.l.) and Taiwa (38°25'24" N, 140°42'35" E, 812 m a.s.l.). On Mt. Izumigatake, *W. hortensis* flowers are mainly visited by bumble bees (*Bombus*, Apidae), small bees (including Andrenidae and Halictidae), hunch-back flies (*Oligoneura* spp., Acroceridae) and hoverflies (Syrphidae) (Chapter II). There are variations in assemblages of flower visitors along the altitudinal gradient; small bees are the predominant visitors at low-altitude sites whereas hunch-back flies increase in relative abundance with increasing altitude (Chapter II).

Pollination effectiveness of flower visitors

From 24 May to 22 June 2022, I performed a field experiment to examine whether flower visits by different taxa of insects resulted in seed production at Yoshinodaira and Taiwa. At each site, 21 *W. hortensis* plants were used in the experiment. On each of 1–3 branches of each plant, 2–7 buds were selected and all anthers in the buds were removed using forceps. This emasculation prevented pollen import by visitors from being influenced by the presence of pollen grains produced by the receiving flower. The branches were then bagged to exclude insects until visit observations were made. After flowering of the emasculated buds, the bags were removed to allow insects to visit the flowers for about 60 min. During this period, insect visits to flowers on each branch were recorded using a digital video camera (HDR-CX420, HDR-CX680, Sony, Japan; GZ-R400, GZ-RX690, JVCKENWOOD, Japan). I marked the emasculated flowers and measured their corolla tube lengths. After 60 min of open pollination, the branches were bagged again until the corollas abscised. Visitor observations were conducted for three days at each site.

In total, visitors to 155 flowers on 33 branches (of 21 plants) at Yoshinodaira and 137 flowers on 36 branches (of 21 plants) at Taiwa were recorded. After fruit maturation, the marked fruits were collected and all seeds in the fruits were counted.

From the video recordings, visitors that contacted stigmas of the emasculated flowers were counted and classified into the following four groups: bumble bees, small bees, hoverflies and hunch-back flies. Small bees possibly included Andrenidae, Halictidae and Apidae although their families were rarely identifiable on the video recordings. Female bumble bees and small bees have pollen transport structures on their hind legs called corbiculae and scopae, respectively (Thorp, 1979). Bumble bee and small bee groups were subdivided according to whether the corbiculae or scopae contacted stigmas, as determined by the video recordings. Since the scopa of a small bee is located around the hind legs, I determined that the inside surfaces of scopae contacted stigmas when small bees climbed on the stigmas.

Morphology and conspecific percentages of pollen carried by insects

From 31 May to 11 June 2021, I sampled visitors to *W. hortensis* flowers at Otaira and Taiwa to compare morphology of *W. hortensis* pollen carried by visitors among pollinator taxa and among body parts within taxa. Bees and flies were captured immediately after leaving *W. hortensis* flowers using plastic vials or a sweep net. Insects captured using a sweep net were then placed into plastic vials. The insects held individually in vials were immediately chilled on ice, transported to the laboratory, preserved at -20°C for one day, and dried with silica gel at room temperature for more than one month. The insects were sent for taxonomic identification by experts after the pollen studies described below.

Pollen was sampled from the dorsal thoraxes of both bees and flies and from the corbiculae/scopae on the tibiae of the bees' hind legs. The dorsal thorax of corbiculate bees is known as one of the 'safe sites', where pollen is less likely to be groomed away than it is from

other body parts (Koch et al., 2017; Tong and Huang, 2018). For analysis with scanning electron microscopy, pollen on each body part of an insect was gently removed with a conductive carbon double-sided tape (5 mm width, Nisshin-EM, Japan) affixed to a cylinder specimen mount (10 mm diameter, Nisshin-EM, Japan). Because corbicular pollen, mixed with regurgitated nectar (Michener, 1999), agglutinated more firmly when dried, it was split in two using forceps, and the section was gently pressed on a double-sided tape. Pollen on specimen mounts was then coated with platinum on an ion sputter coater (E-1045, Hitachi High-Tech, Japan) and observed using a scanning electron microscope (S-3400N, Hitachi High-Tech, Japan) at 3.0 kV. For each specimen mount, approximately eight *W. hortensis* pollen grains were randomly selected and photographed at 1000x. Then, the diameters and spine lengths of pollen grains in the images were measured using a program developed in Mathematica 11.1 (Wolfram Research, 2017). The diameter of a pollen grain was defined as the diameter of the inscribed circle inside its outline. The spine length was defined as the mean length of the five longest spines forming a part of the outline of the pollen grain. In addition, to compare pollen traits between pollen on insects and in flowers, I reanalyzed images of pollen grains sampled from flowers (Chapter II). These images were collected in 2020 at the same sites used in this study. Pollen was sampled from five fresh flowers of each of ten individual plants at each site, and six to ten pollen grains from each flower were photographed (Chapter II).

Pollen carried by insects captured on *W. hortensis* flowers originated not only from *W. hortensis* flowers but also from heterospecific flowers. The percentages of *W. hortensis* pollen grains were estimated as one of the factors influencing pollination efficiency of insect visitors. For each specimen mount, three or four images of pollen grains were taken at 100x or 200x using a scanning electron microscope to include as many pollen grains as possible regardless of donor species. Up to 50 pollen grains for each specimen mount were classified according to whether they were *W. hortensis* or heterospecific. For specimen mounts with sparse pollen, I

counted all *W. hortensis* and heterospecific pollen grains without taking images.

Statistical analyses

All statistical models were developed in PyMC3, a Python probabilistic programming framework for Bayesian parameter estimation (Salvatier et al., 2016). In all Bayesian statistical analyses described below, the No-U-Turn Sampler was used to generate four Markov chain Monte Carlo (MCMC) chains each with 10,000 iterations following a burn-in period of 10,000 iterations. The potential scale reduction factors (R-hat) were below 1.01 for all parameters, indicating convergence of the MCMC chains. Variance inflation factors in the models with multiple predictors were at most 1.25, suggesting that there were no problems of multicollinearity (Dormann et al., 2013). The fieldwork was done at multiple study sites, so I developed separate statistical models for each site.

I ran multiple regressions to test for the effect of visits by different visitor groups on seed production. I used the visit and seed data for flowers receiving at least one visit with a stigma contact. However, I excluded the data for flowers on branches that did not produce any fruits with seeds, as these branches may have lacked energy. As a result, the visit and seed data for 40 fruits (on 16 branches of 12 plants) at Yoshinodaira and 96 fruits (on 30 branches of 19 plants) at Taiwa were analyzed. The multiple regression models included the number of seeds per fruit as an outcome variable and the number of visits with stigma contacts by different visitor groups and standardized corolla tube length as predictors. For bees, visits with stigma contacts by bodies or by corbiculae/scopae were included as separate predictors. The models also included branches as a random factor to account for repeated measures. Although I observed insect visits to 1–3 branches on the same plants, plants were not held as a random factor because only one branch was used for eight out of 12 plants at Yoshinodaira and 12 out of 19 plants at Taiwa. A negative binomial sampling distribution was used with a log link

function.

To compare pollen traits among pollen sources, I developed statistical models estimating the means and standard deviations of trait distributions of pollen grains from different pollen sources. The estimations for pollen sampled from insects were performed with a single model that included individual insects as a random factor. The models for pollen from flowers included plants and flowers as random factors. For pairwise comparisons between pollen sources, posterior distributions of differences between the means of trait distributions were estimated for all pairs of pollen sources using the MCMC samples. A gamma sampling distribution was used for both pollen grain spine length and pollen grain diameter.

To test for the effects of pollen traits on the probability of pollen collection from the bodies to the corbiculae/scopae of bees, I ran separate multiple logistic regressions by the bee group. I used only the pollen data where pollen was sampled from both the bodies and corbiculae/scopae of the same individual bees. The multiple regression models included whether pollen was collected or not as an outcome variable (1.0 for pollen collected into the corbiculae/scopae, and 0.0 for pollen remaining on the bodies), standardized spine length and diameter as predictors and the interaction of the predictors. I also incorporated the quadratic terms of both predictors in the models to distinguish whether the collection probability was highest at an extreme or intermediate pollen trait. When the estimate of a quadratic term was negative, I estimated an intermediate pollen trait value achieving the highest collection probability using the MCMC samples. The regression models also included individual bees as a random factor. A Bernoulli sampling distribution was used with a logit link function.

To compare *W. hortensis* pollen percentages among pollen sources, I developed statistical models estimating *W. hortensis* pollen percentages from different pollen sources. A beta-binomial sampling distribution, which allowed me to account for overdispersed count data (Gelman and Hill, 2007), was applied to the numbers of *W. hortensis* and heterospecific pollen

grains with a logit link function. The estimations for pollen sampled from pollen sources to be compared were performed with a single model. For pairwise comparisons between pollen sources, posterior distributions of differences between the *W. hortensis* pollen percentages were estimated for all pairs of pollen sources using the MCMC samples.

Results

Pollination effectiveness of flower visitors

For flowers visited by insects at least once during a 60-min pollination period, the number of seeds per fruit was 10 ± 17 (mean \pm s.d., $n = 40$) at Yoshinodaira and 19 ± 17 ($n = 96$) at Taiwa. At Yoshinodaira, bumble bees ($n = 7$), small bees ($n = 143$) and hoverflies ($n = 4$) were observed visiting *W. hortensis* flowers (Table III-1). During visits, the bodies of all three groups and the scopae of small bees contacted stigmas. In total 72 visits included stigma contacts, and the bodies of small bees contacted stigmas most frequently ($n = 32$, 44.4%), followed by the scopae of small bees ($n = 30$, 41.7%), the bodies of bumble bees ($n = 7$, 9.7%), and the bodies of hoverflies ($n = 3$, 4.2%). At Yoshinodaira, visits with stigma contacts by the scopae of small bees had a positive effect on seed production (Table III-2). The model-estimated median of the coefficient was 1.241, indicating that the number of seeds per fruit increased by $\exp(1.241) \approx 3.46$ times with a single visit including a stigma contact by the scopa of a small bee. At Taiwa, bumble bees ($n = 152$), small bees ($n = 260$), hunch-back flies ($n = 196$) and hoverflies ($n = 43$) were observed as visitors (Table III-1). During visits, the bodies of all four groups and the corbiculae/scopae of the bees contacted stigmas. In total 459 visits included stigma contacts, and the bodies of bumble bees contacted stigmas most frequently ($n = 133$, 29.0%), followed by the bodies of hunch-back flies ($n = 124$, 27.0%), the bodies of small bees ($n = 78$, 17.0%), the scopae of small bees ($n = 77$, 16.8%), the bodies of hoverflies ($n = 35$, 7.6%), and the corbiculae of bumble bees ($n = 12$, 2.6%). At Taiwa, visits with stigma contacts by the bodies

of bumble bees and hunch-back flies had positive effects on seed production (Table III-2). The model-estimated medians of the coefficients were 0.205 and 0.137, indicating that the number of seeds per fruit increased by approximately 1.23 and 1.15 times with a single visit including a stigma contact by the body of a bumble bee or a hunch-back fly, respectively. At Taiwa, the number of seeds per fruit also increased with increased corolla tube length (Table III-2).

Morphology and conspecific percentages of pollen carried by insects

At Otaira and Taiwa, the following insects were collected (Table III-3): bumble bees (*Bombus diversus*, *B. honshuensis*, *B. ardens* and *B. hypocrite*, Apidae), andrenid bees (*Andrena lonicerae*, Andrenidae), halictid bees (*Lasioglossum* spp., Halictidae) and hunch-back flies (*Oligoneura nigroaenea*, Acroceridae). Of the bumble bees collected, 19 were females and three were males from Otaira, while six were females and seven were males from Taiwa. Corbicular pollen was found on 17 out of the 19 female bumble bees at Otaira and four out of the six female bumble bees at Taiwa. Scopal pollen was found on 22 out of 25 andrenid bees at Otaira and all 13 andrenid bees and three out of eight halictid bees at Taiwa. None of the seven halictid bees at Otaira had pollen on the tibial scopae. Due to small sample sizes, I did not conduct analyses involving corbicular pollen on bumble bees at Taiwa or pollen on halictid bees at either site.

Pollen grain spine length and pollen grain diameter were compared among the bodies of bumble bees, the scopae of andrenid bees and the bodies of hunch-back flies, the visitor groups identified as effective in seed production in my field experiment (Table III-2). At both study sites, the spine length of pollen grains on the bodies of bumble bees was greater than the spine lengths of pollen grains on the scopae of andrenid bees or the bodies of hunch-back flies (Fig. III-1a, b). Pollen grains on these pollinator groups had shorter spines than pollen grains in flowers at both sites (Fig. III-1a, b). At Otaira, the diameters of pollen grains on the scopae of

andrenid bees and the bodies of bumble bees were larger than the diameter of pollen grains on the bodies of hunch-back flies (Fig. III-1c). At Taiwa, pollen grains on the scopae of andrenid bees were larger in diameter than pollen grains on the bodies of bumble bees or hunch-back flies (Fig. III-1d). Pollen grains on the bodies of bumble bees at Taiwa and pollen grains on the bodies of hunch-back flies at both sites were smaller than pollen grains in flowers at the corresponding sites (Fig. III-1c, d). Pairwise comparisons including pollen sources that hardly contributed to seed production were also conducted; the bodies of andrenid bees had pollen grains with shorter spines and smaller diameters than the bodies of bumble bees at Otaira but these differences were not found at Taiwa (see Fig. III-2a–d for details).

The probability that pollen was collected from the bodies to the corbiculae of bumble bees at Otaira increased with decreasing spine length and increasing diameter (Fig. III-3a, b; Table III-4). The probability of pollen collection into the scopae of andrenid bees at Taiwa tended to increase with decreasing spine length, but not diameter (Fig. III-3e, f; Table III-4). Spine length hardly influenced the probability of pollen collection into the scopae of andrenid bees at Otaira (Fig. III-3c; Table III-4). However, the quadratic term of pollen grain diameter was negative (Table III-4), indicating that pollen with an intermediate diameter had the highest probability of being collected into the scopae (Fig. III-3d). The model-estimated median of the diameter associated with the highest collection probability was 38.40 μm (95% highest density interval (HDI): 37.54–39.53 μm), which was larger than the mean diameter of pollen grains on the bodies of andrenid bees at Otaira (37.41 μm ; Table III-3).

Compared among the pollinator groups, the percentage of *W. hortensis* pollen was the highest on the scopae of andrenid bees at both sites ($99.55 \pm 1.7\%$ at Otaira and $98.46 \pm 2.5\%$ at Taiwa, mean \pm s.d.; Fig. III-1e, f; Table III-3). At Otaira, there was no significant difference in the *W. hortensis* pollen percentage between the bodies of hunch-back flies ($95.68 \pm 7.66\%$) and the bodies of bumble bees ($93.15 \pm 9.94\%$) (Fig. III-1e; Table III-3). At Taiwa, the *W.*

hortensis pollen percentage on the bodies of hunch-back flies ($90.3 \pm 18.66\%$) was higher than on the bodies of bumble bees ($79.95 \pm 29.55\%$) (Fig. III-1f; Table III-3). Comparisons of the *W. hortensis* pollen percentages relative to all pollen sources showed that the percentages on the bodies of andrenid bees were higher than on the bodies of bumble bees, while pollen on the corbiculae of bumble bees had the lowest percentage (Fig. III-2e, f).

Discussion

Pollination effectiveness of flower visitors

The field experiment suggested that different pollinators carried *W. hortensis* pollen from anthers to stigmas at the two study sites, Yoshinodaira and Taiwa. At Yoshinodaira, only pollen on the scopae of small bees contributed to seed production (Table III-2). Most andrenid bees captured on *W. hortensis* flowers carried a lot of pollen on their scopae, where pollen remains dry and loose without mixing with nectar, whereas only a few halictid bees carried pollen on their scopae. Pollen is probably held viably on the scopae as Parker et al. (2015) demonstrated that scopal pollen has the same ability to fertilize ovules as pollen on bee bodies. Additionally, I found that andrenid bees are faithful to *W. hortensis* flowers as the percentages of *W. hortensis* pollen on the scopae of andrenid bees were more than 98%, the highest among pollinator groups (Fig. III-1e, f; Table III-3). Therefore, at least in environments where flowers are predominantly visited by small bees, they, especially andrenid bees, are presumably effective pollinators of *W. hortensis* flowers. Therefore, *W. hortensis* pollen morphology could be subject to selection to facilitate pollen collection on the scopae of andrenid bees.

On the other hand, at Taiwa, where small bees, bumble bees and hunch-back flies visited flowers at similar frequencies (Table III-1), stigma contacts with the scopae of small bees had little effect on the number of seeds produced (Table III-2). Alternatively, pollen on the bodies of bumble bees and hunch-back flies contributed to seed production (Table III-2). Bumble bees

and hunch-back flies may be more efficient pollinators of *W. hortensis* than small bees. Hunch-back flies are distinctly different from bees in terms of morphology and behavior; they have a lower level of hairiness than bees, feed on nectar but not pollen in *W. hortensis* flowers and do not groom body pollen (personal observation). In addition, hunch-back flies were more faithful to *W. hortensis* flowers than bumble bees as indicated by the *W. hortensis* pollen percentages on their bodies (Fig. III-1f; Table III-3). Comparison of the regression coefficients suggested that bumble bees and hunch-back flies were not greatly different in pollination efficiency (Table III-2), reflecting the fact that hunch-back flies consistently foraged for nectar but not pollen of *W. hortensis* flowers. Morphology of *W. hortensis* pollen could be subject to selection to facilitate adhesion to the bodies of bumble bees and hunch-back flies in environments such as Taiwa, where these pollinators are abundant.

Pollen grain spine length for successful pollination

The comparison analyses of morphology of pollen carried by different pollinator groups showed that the pollen morphology that promotes successful pollination depends on pollinator taxa. Pollen grains on the bodies of bumble bees had longer spines than pollen grains on the scopae of andrenid bees or the bodies of hunch-back flies at both study sites, Otaira and Taiwa (Fig. III-1a, b). This suggests that pollination by bumble bees is facilitated by longer pollen spines than pollination by andrenid bees or hunch-back flies. The differences in spine length between them may reflect their different levels of hairiness, which could influence the degree of pollen grain anchoring (Thorp, 1979), and a common tendency for bumble bees and andrenid bees to collect pollen grains with shorter spines (Fig. III-3a, e). This tendency is consistent with the results of previous work that compared the collectability of pollen from multiple species for corbiculate bees (bumble bees or honey bees) (Lunau et al., 2015; Vaissière and Vinson, 1994). For the first time, I provided evidence that the tendency to collect pollen grains with shorter

spines is common to corbiculate bees and non-corbiculate, andrenid bees.

Weigela hortensis flowers produced pollen grains with spine lengths longer than those facilitating adhesion to pollinators (Fig. III-1a, b). Pollen spines could also affect pollination processes beyond pollen adhesion to a pollinator, such as pollen transfer from a pollinator to a stigma. For example, in *Helianthus annuus* (Asteraceae), interlocking between pollen spines and stigma papillae enhances adhesion of a pollen grain to a stigma (Lin et al., 2016). Alternatively, pollen spines could accumulate electric charge and influence electrostatic forces between a pollen grain and a stigma (Inchaussandague et al., 2018). The effects of pollen spine phenotypes on the probability that pollen on a pollinator is transferred to and retained on a stigma should be examined in future studies.

Pollen grain diameter for successful pollination

Pollen grains on the scopae of andrenid bees had larger diameters than pollen grains on the bodies of hunch-back flies at both study sites (Fig. III-1c, d), suggesting that pollination by andrenid bees could be facilitated by larger pollen compared to pollination by hunch-back flies. This may result from the tendency of andrenid bees to collect pollen with a slightly larger diameter than the mean diameter of body pollen (Fig. III-3d). The pollen diameter giving a high probability of pollen collection by andrenid bees might ensure a mechanical fit between branched hairs of the scopae (Amador et al., 2017; Thorp, 1979; Thorp, 2000). In contrast, bumble bees collected larger pollen more easily (Fig. III-3b). As Harder (1998) proposed, larger pollen could be more easily groomed with the comb-like structures on bees' legs. Although Harder (1998) did not find evidence supporting this hypothesis by comparing pollen grain size between plant species with pollinators that exhibit different grooming behavior, my survey provided evidence by directly examining the effect of intraspecific quantitative variation in pollen grain diameter on pollen collectability. This finding seems to disagree with the result of

Hao et al. (2020) showing that pollen grain diameter was larger in plant species from which bees did not collect pollen than in plant species from which bees did collect pollen. However, as Hao et al. (2020) indicated, their result might reflect the possibility that selection is actually on pollen number, which negatively correlates with pollen size.

Pollen grains on the bodies of bumble bees were larger or smaller than pollen grains on the other groups, depending on the study site (Fig. III-1c, d). Bumble bees were collected from different castes of four species with different morphology or behavior that can affect interaction with pollen morphology. As males of *B. ardens* accounted for seven out of 13 samples at Taiwa, there might be sampling bias due to altitudinal variation in species or castes of pollinating bumble bees (Kuriya et al., 2015; Toji et al., 2021). Further work is required to determine whether the diameter giving pollen grains high stickiness to bumble bee bodies depends on bumble bee species or castes.

Conclusions

I showed that *W. hortensis* pollen morphology that promotes successful pollination depends on pollinator taxa. The differences in pollen grain spine length and pollen grain diameter between pollinators from different taxa reflected pollen collection from bodies to pollen transport structures by bees. Morphological traits of specific pollinators may also have had an effect. This study extends the knowledge of interactions between pollen and pollinators and raises the possibility that pollen morphology has diversified to facilitate the success of pollination by a variety of pollinating partners. Variation in pollen morphology in a generalist plant may ensure reproductive success. Further studies that associate pollen morphology with pollen deposition on a stigma and post-pollination success will improve our understanding of the diversity of pollen morphology.

Table III-1. The number of visitors contacting a stigma per flower during an approximately 60-min period. The visit data for flowers receiving at least one insect visit with a stigma contact were used. Means \pm s.d. are shown.

Site	Visitor group	Visit number
Yoshinodaira	Bumble bee (body)	0.18 \pm 0.38
	Bumble bee (corbicula)	0
	Small bee (body)	0.75 \pm 0.92
	Small bee (scopa)	0.80 \pm 0.75
	Hunch-back fly	0
	Hoverfly	0.08 \pm 0.35
Taiwa	Bumble bee (body)	1.39 \pm 1.24
	Bumble bee (corbicula)	0.13 \pm 0.36
	Small bee (body)	0.81 \pm 1.23
	Small bee (scopa)	0.80 \pm 1.09
	Hunch-back fly	1.29 \pm 1.72
	Hoverfly	0.36 \pm 0.68

Table III-2. Posterior coefficient estimates from Bayesian multiple regression models testing for the effect of visits to *Weigela hortensis* flowers by different visitor groups on seed production. All estimated coefficients are listed as the median with the 95% highest density interval (HDI) in parentheses. At Yoshinodaira, the corbiculae of bumble bees were not observed to contact stigmas.

Site	Predictor	Coefficient estimate
Yoshinodaira	Bumble bee (body)	0.269 (−1.609, 2.188)
	Small bee (body)	0.097 (−0.545, 0.748)
	Small bee (scopa)	1.241 (0.108, 2.383)
	Hoverfly	−1.709 (−3.593, 0.415)
	Corolla tube length	0.360 (−0.281, 1.017)
Taiwa	Bumble bee (body)	0.205 (0.018, 0.399)
	Bumble bee (corbicula)	0.305 (−0.322, 0.948)
	Small bee (body)	−0.081 (−0.275, 0.109)
	Small bee (scopa)	0.033 (−0.145, 0.214)
	Hunch-back fly	0.137 (0.020, 0.261)
	Hoverfly	0.268 (−0.072, 0.602)
	Corolla tube length	0.404 (0.116, 0.712)

Table III-3. Spine length, diameter and conspecific percentage of *Weigela hortensis* pollen grains sampled from various pollen sources. Means \pm s.d. are shown.

Site	Pollen source	Spine length (μm)	Diameter (μm)	Conspecific percentage (%)	Pollen (insect/flower) sample size
Otaira	Bumble bee (body)	2.56 \pm 0.49	37.92 \pm 3.15	93.15 \pm 9.94	168 (22)
	Bumble bee (corbicula)	2.27 \pm 0.43	40.21 \pm 2.24	71.11 \pm 39.82	124 (17)
	Andrenid bee (body)	2.48 \pm 0.44	37.41 \pm 2.19	98.64 \pm 2.98	192 (25)
	Andrenid bee (scopa)	2.45 \pm 0.45	37.68 \pm 1.81	99.55 \pm 1.70	172 (22)
	Halictid bee (body)	2.55 \pm 0.41	37.14 \pm 2.15	49.05 \pm 44.15	39 (7)
	Hunch-back fly	2.48 \pm 0.45	36.43 \pm 2.51	95.68 \pm 7.66	245 (33)
	Flower	2.73 \pm 0.47	37.92 \pm 2.34	—	359 (50)
Taiwa	Bumble bee (body)	2.5 \pm 0.45	37.17 \pm 2.72	79.95 \pm 29.55	91 (13)
	Bumble bee (corbicula)	2.05 \pm 0.49	39.35 \pm 2.73	45.06 \pm 42.12	9 (4)
	Andrenid bee (body)	2.47 \pm 0.49	37.38 \pm 2.68	92.15 \pm 24.34	94 (13)
	Andrenid bee (scopa)	2.35 \pm 0.44	37.68 \pm 2.32	98.46 \pm 2.50	101 (13)
	Halictid bee (body)	2.66 \pm 0.37	37.3 \pm 2.39	72.09 \pm 28.07	49 (8)
	Halictid bee (scopa)	2.71 \pm 0.31	38.47 \pm 1.40	82.00 \pm 17.05	24 (3)
	Hunch-back fly	2.33 \pm 0.40	36.79 \pm 2.73	90.3 \pm 18.66	190 (27)
	Flower	2.76 \pm 0.49	37.9 \pm 2.33	—	360 (50)

Table III-4. Posterior coefficient estimates from Bayesian multiple logistic regression models examining the effects of pollen grain spine length and diameter on the probability of pollen collection from bodies to corbiculae/scopae of bees. All estimated coefficients are listed as the median with the 95% highest density interval (HDI) in parentheses. Due to the small sample size, a regression analysis for bumble bees at Taiwa was not conducted.

Site	Pollen source	Predictor	Coefficient estimate
Otaira	Bumble bee	Spine length	-0.860 (-1.256, -0.499)
		Spine length ²	0.046 (-0.189, 0.285)
		Diameter	1.146 (0.763, 1.518)
		Diameter ²	-0.171 (-0.468, 0.112)
		Interaction	-0.185 (-0.561, 0.220)
	Andrenid bee	Spine length	-0.105 (-0.319, 0.117)
		Spine length ²	0.009 (-0.151, 0.166)
		Diameter	0.124 (-0.104, 0.349)
		Diameter ²	-0.146 (-0.298, -0.012)
		Interaction	-0.058 (-0.273, 0.163)
Taiwa	Andrenid bee	Spine length	-0.283 (-0.603, 0.029)
		Spine length ²	-0.033 (-0.235, 0.151)
		Diameter	0.098 (-0.213, 0.410)
		Diameter ²	-0.100 (-0.295, 0.085)
		Interaction	0.092 (-0.237, 0.437)

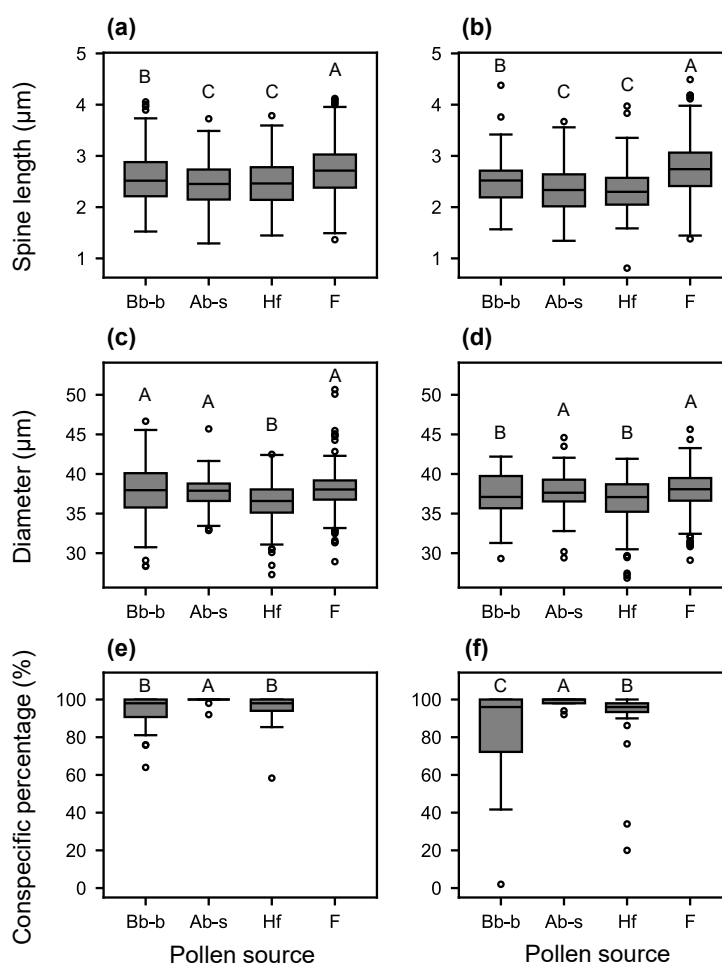


Fig. III-1. (a, b) Spine length, (c, d) diameter and (e, f) conspecific percentage of *Weigela hortensis* pollen grains sampled from flowers and the visitor groups identified as effective in seed production. Insects were captured immediately after leaving *W. hortensis* flowers at the two study sites, (a, c, e) Otaira and (b, d, f) Taiwa. In each panel, pollen sources sharing a letter were not significantly different, i.e., the 95% highest density interval (HDI) of the difference of the means derived from Bayesian models did not exclude zero. Pollen sources: (Bb-b) bodies of bumble bees, (Ab-s) scopae of andrenid bees, (Hf) bodies of hunch-back flies, and (F) flowers.

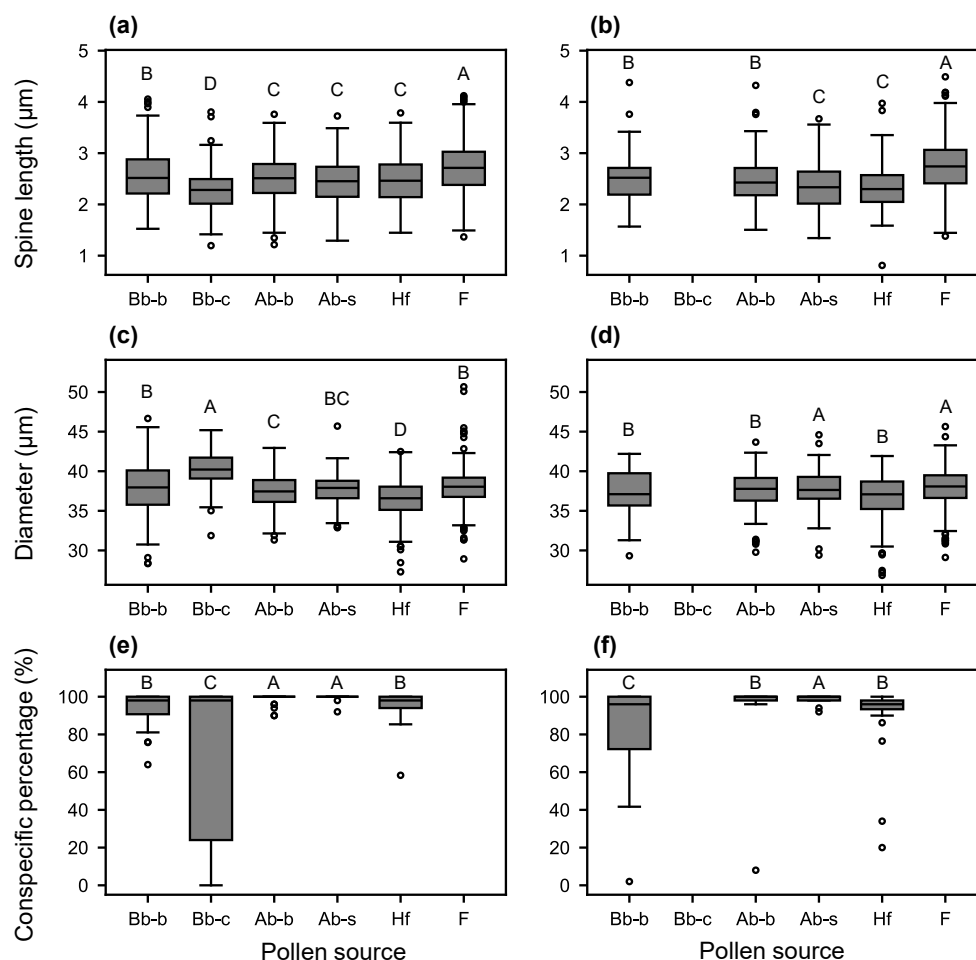


Fig. III-2. (a, b) Spine length, (c, d) diameter and (e, f) conspecific percentage of *Weigela hortensis* pollen grains sampled from flowers and insects. Insects were captured immediately after leaving *W. hortensis* flowers at the two study sites, (a, c, e) Otaira and (b, d, f) Taiwa. In each panel, pollen sources sharing a letter were not significantly different, i.e., the 95% highest density interval (HDI) of the difference of the means derived from Bayesian models did not exclude zero. Due to small sample sizes, corbicular pollen on bumble bees at Taiwa and pollen on halictid bees at both sites were excluded from the comparison analyses. Pollen sources: (Bb-b) bodies of bumble bees, (Bb-c) corbiculae of bumble bees, (Ab-b) bodies of andrenid bees, (Ab-s) scopae of andrenid bees, (Hf) bodies of hunch-back flies, and (F) flowers.

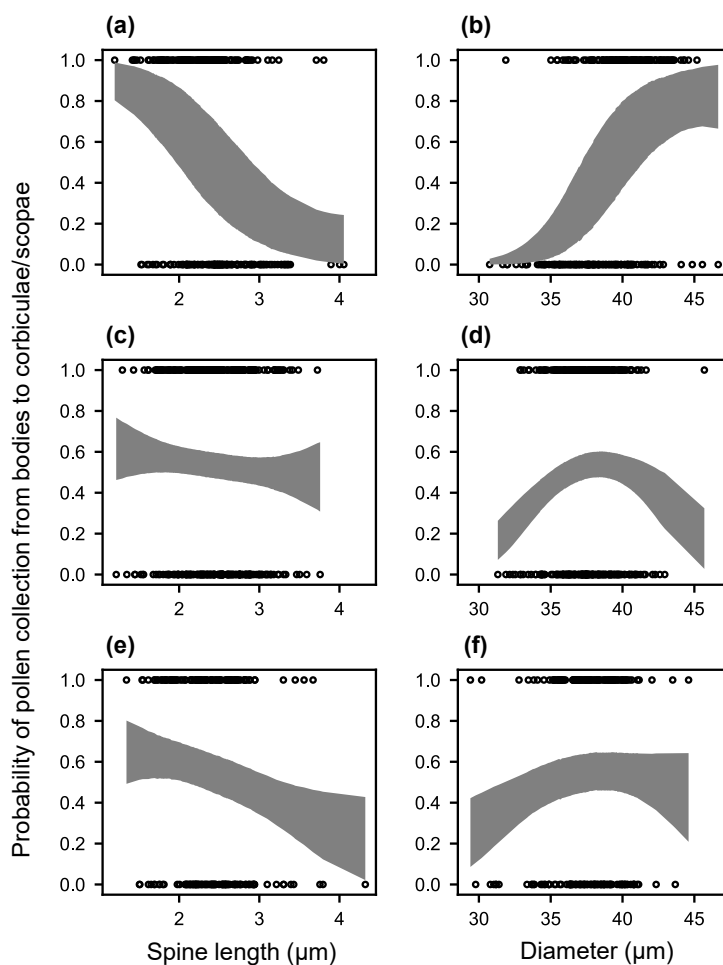


Fig. III-3. The effects of pollen grain spine length and diameter on the probability of pollen collection from bodies to corbiculae/scopae of bees. (a, b) bumble bees at Otaira, (c, d) andrenid bees at Otaira, and (e, f) andrenid bees at Taiwa. Multiple logistic regressions incorporating the quadratic terms of predictors were conducted. On the vertical axis, 1.0 represents pollen collected into corbiculae/scopae, and 0.0 represents pollen remaining on bodies. The 95% highest density intervals (HDIs) of the collection probabilities were derived from Bayesian models that held the other predictor constant at their mean values and included individual insects as a random factor. Due to the small sample size, a regression analysis for bumble bees at Taiwa was not conducted.

General Discussion

Overview of findings

In this thesis, I demonstrated that pollen morphology has a great impact on pollination success and evolves depending on pollinator taxa. In Chapter I, using a theoretical model, I found that pollen morphology relating to stickiness to pollinators influenced the number of pollen recipient flowers and overall pollen deposition (the overall number of pollen grains deposited on stigmas of recipient flowers) and was selected on the trade-off between them. While several studies suggest that pollen spines and pollenkitt play important roles in adhesion between pollen grains and a pollinator body (e.g., Amador et al., 2017; Berger et al., 1988; Lin et al., 2013; Pacini and Hesse, 2005), I disclosed the benefits of enhanced adhesion for plant reproductive success and pollinator characteristics that selected for sticky pollen. In Chapter II, I examined intraspecific quantitative variations in the morphology of *Weigela hortensis* pollen grains and found that spine length differed between sites with different pollinator assemblages. Although interspecific correlations between pollen morphology and pollinator taxa have been well documented (e.g., Hemsley and Ferguson, 1985; Sannier et al., 2009; Stroo, 2000), I have provided evidence of an intraspecific correlation for the first time. In Chapter III, I demonstrated the effects of spine length and diameter of *W. hortensis* pollen grains on successful pollination by a variety of pollinators. Interactions between pollen morphology and pollinator foraging behavior or morphology influenced adhesion of pollen grains to pollinator body parts where pollen transfer to stigmas can occur. The differences in pollen grain spine length facilitating pollination by local pollinators may lead to the differentiation in spine length along an altitudinal gradient.

In summary, this thesis extends an understanding of the evolution of pollen morphology facilitating pollination success by studying (i) the effect of pollen morphology on the likelihood of adhesion between pollen grains and a pollinator (Chapter III), (ii) the benefits of enhanced adhesion between them for male reproductive success (Chapter I), (iii) pollinator characteristics that exert strong selection favoring stickier pollen (Chapter I) and (iv) the intraspecific

differentiation in pollen morphology driven by the altitudinal difference in local pollinator assemblages (Chapters II and III).

Model prediction and field observation

In Chapter I, I established a simple model to predict the dispersal patterns of pollen varying in stickiness to pollinators. This model provides an insight into pollinator characteristics that exert strong selection favoring stickier pollen. According to the model prediction, there are two main conditions where selection favoring stickier pollen is strong (see *Pollen stickiness evolution dependent on pollinating partners* in Results and Discussion of Chapter I).

The first condition is when pollinators move limited distances in a given time and are likely to revisit flowers that they have previously visited. In the study sites of Chapters II and III, the probability of revisits to the same flowers seemed very low for all pollinators because individual *W. hortensis* plants have a lot of flowers. However, since the flowers are self-incompatible, sticky pollen may also be selected for by pollinators with a low probability of departing a plant after visiting a flower although I did not compare the probability between pollinator taxa.

The second condition is when pollen is likely to be lost during transport. In the *W. hortensis* pollination system, this kind of pollinators could be bumble bees, which collected pollen from bodies to corbiculae where pollen is not useful for pollination. For impeding pollen collection on the corbiculae, longer spines, which seem to have a higher cost, may be strongly selected for by bumble bees (Chapter III). Similarly, because pollen remaining on the bodies of andrenid bees without collected on the scopae has little chance of stigma deposition (Chapter III), there could be strong selection for shorter spines and diameter associated with the highest probability of collection on the scopae (Chapter III). Since the probability of pollen loss during transport depends largely on the intensity and frequency of pollen grooming, comparison of the

probability between pollinator taxa will improve our understanding of the diversification in pollen morphology.

Model predictions are useful for understanding the basic mechanisms of evolution, but in actual pollination systems, there are various ecological contexts that differ from the simple assumptions of the models. To predict evolution in pollination systems with multiple pollen routes from anthers to stigmas, such as in *W. hortensis*, models that take into account the realistic conditions are necessary.

Pollen morphological differentiation in a generalist plant

In Chapter II, I showed that on Mt. Izumigatake spine length of *W. hortensis* pollen grains was greater at higher-altitude sites, and small bees were the predominant visitors at low-altitude sites whereas hunch-back flies increased in relative abundance with increasing altitude. Can this altitudinal variation be explained by the differences in pollen grain spine length facilitating pollination by local pollinators found in Chapter III? The finding that andrenid bees collected pollen grains with shorter spines on their scopae supports the idea that the altitudinal variation in pollen grain spine length is the result of selection favoring shorter spines exerted by low-altitudinal pollinators. However, contrary to my expectation, the mean spine length of pollen grains collected on the scopae of andrenid bees was not significantly smaller than that of pollen on hunch-back flies. Therefore, I cannot confidently conclude that the altitudinal variation in spine length has resulted from the difference in local pollinator assemblages. Nevertheless, andrenid bees and hunch-back flies could exert different selection pressures on spine length. Theoretical work in Chapter I suggests that the strength of selection toward highest pollen stickiness to pollinators can vary according to pollinator taxa given the cost of producing pollen sticking elements such as spines. This is because pollen grooming intensity or foraging areas of pollinators may influence the rate of plant fitness return on the production of costly sticking

elements. Thus, even though the same pollen grain spine length facilitates pollination by two different pollinators, they could select for different spine lengths and cause the altitudinal variation.

Whereas pollen grain diameter for successful pollination depended on pollinator taxa, altitudinal variation in pollen grain diameter was not found. Pollen grain size may influence reproductive success not only in the pollination process but also in post-pollination processes. During post-pollination processes, large pollen grains may outperform small ones in pollen competition for ovule fertilization (McCallum and Chang, 2016). In that case, there would be an optimal pollen grain size maximizing success in post-pollination processes under pollen grain size-number trade-offs (Smith and Fretwell, 1974; Vonhof and Harder, 1995). Therefore, pollen grain size could be under stabilizing selection in post-pollination processes, and the pollen grain size optimal for the pollination process may not necessarily have been selected for. For a better understanding of pollen grain size evolution in *W. hortensis*, the effect of pollen grain size on post-pollination success should be examined in future studies.

Significance of pollen morphology as a reproductive strategy

Pollen grain size, pollen spines and pollenkitt determine the fates of pollen grains. These pollen morphological traits govern the force of adhesion to a pollinator body (Amador et al., 2017; Berger et al., 1988; Lin et al., 2013; Pacini and Hesse, 2005). Thus, they can decrease the probability of passive pollen loss from a pollinator body during transport. They can also change the probability of pollen collection on transport structures by bees (Chapter III; Amador et al., 2017; Konzmann et al., 2019; Lunau et al., 2015); selection sometimes favors pollen morphology impeding collection by corbiculate bees and sometimes favors pollen morphology facilitating collection by bees whose scopal pollen is useful for pollination (Chapters II and III). Reduced pollen loss increases pollen recipient number and overall pollen deposition (Chapter

I).

Successful pollination via pollinating partners is vital to plant reproductive success. Although flowers have a variety of strategies operating when pollen is removed from anthers (reviewed in Minnaar et al., 2019), pollen morphology should be one of the few strategies operating after departure from anthers. Pollen morphology may have diversified as a strategic trait that cannot be replaced by other floral traits.

Acknowledgements

I would like to express my deepest gratitude to Associate Professor Satoki Sakai for generous support during my six years in his laboratory. I would also like to thank Professor Michio Kondoh, Masayuki Maki and Satoshi Chiba for reviewing this thesis. I am grateful to Tomoyuki Itagaki and Takashi Makino for continuous support throughout this study, Michio Oguro for advice about statistical analyses, Masatoshi Tanno for technical support in operating the scanning electron microscope, Koji Yonekura for his expertise in educating me on plant classification and distribution and Jane Glazebrook for editing the language. The advice and fieldwork assistance from the members of Ecological Integration laboratory, Plant Ecology laboratory and Functional Ecology laboratory were also helpful. Lastly, I would like to thank my family for support and encouragement during my student life.

References

- Aigner, P.A. (2004) Floral specialization without trade-offs: Optimal corolla flare in contrasting pollination environments. *Ecology*, **85**(9), 2560-2569.
- Amador, G.J., Matherne, M., Waller, D., Mathews, M., Gorb, S.N., Hu, D.L. (2017) Honey bee hairs and pollenkitt are essential for pollen capture and removal. *Bioinspiration & Biomimetics*, **12**(2).
- Anderson, B., Ros, P., Wiese, T.J., Ellis, A.G. (2014) Intraspecific divergence and convergence of floral tube length in specialized pollination interactions. *Proceedings of the Royal Society B-Biological Sciences*, **281**(1795).
- Basso-Alves, J.P., Agostini, K., Teixeira, S.P. (2011) Pollen and stigma morphology of some Phaseoleae species (Leguminosae) with different pollinators. *Plant Biology*, **13**(4), 602-610.
- Berger, L.A., Vaissiere, B.E., Moffett, J.O., Merritt, S.J. (1988) *Bombus* spp. (Hymenoptera, Apidae) as pollinators of male-sterile upland cotton on the Texas high plains. *Environmental Entomology*, **17**(5), 789-794.
- Byars, S.G., Parsons, Y., Hoffmann, A.A. (2009) Effect of altitude on the genetic structure of an Alpine grass, *Poa hiemata*. *Annals of Botany*, **103**(6), 885-899.
- Castellanos, M.C., Wilson, P., Keller, S.J., Wolfe, A.D., Thomson, J.D. (2006) Anther evolution: Pollen presentation strategies when pollinators differ. *American Naturalist*, **167**(2), 288-296.
- Castellanos, M.C., Wilson, P., Thomson, J.D. (2003) Pollen transfer by hummingbirds and bumblebees, and the divergence of pollination modes in *Penstemon*. *Evolution*, **57**(12), 2742-2752.
- Codling, E.A., Plank, M.J., Benhamou, S. (2008) Random walk models in biology. *Journal of the Royal Society Interface*, **5**(25), 813-834.
- Conner, J.K. and Rush, S. (1996) Effects of flower size and number on pollinator visitation to

- wild radish, *Raphanus raphanistrum*. *Oecologia*, **105**(4), 509-516.
- Dobson, H.E.M. (1988) Survey of pollen and pollenkitt lipids - chemical cues to flower visitors. *American Journal of Botany*, **75**(2), 170-182.
- Dormann, C.F., Elith, J., Bacher, S., Buchmann, C., Carl, G., Carre, G., Marquez, J.R.G., Gruber, B., Lafourcade, B., Leitao, P.J., Munkemuller, T., McClean, C., Osborne, P.E., Reineking, B., Schroder, B., Skidmore, A.K., Zurell, D., Lautenbach, S. (2013) Collinearity: a review of methods to deal with it and a simulation study evaluating their performance. *Ecography*, **36**(1), 27-46.
- Ejsmond, M.J., Ejsmond, A., Banasiak, L., Karpinska-Kolaczek, M., Kozłowski, J., Kolaczek, P. (2015) Large pollen at high temperature: an adaptation to increased competition on the stigma? *Plant Ecology*, **216**(10), 1407-1417.
- Faegri, K. and van der Pijl, L. (1979) *The principles of pollination ecology* Pergamon Press, Oxford.
- Fetscher, A.E. (2001) Resolution of male-female conflict in an hermaphroditic flower. *Proceedings of the Royal Society B-Biological Sciences*, **268**(1466), 525-529.
- Fromhage, L. and Kokko, H. (2010) Spatial seed and pollen games: dispersal, sex allocation, and the evolution of dioecy. *Journal of Evolutionary Biology*, **23**(9), 1947-1956.
- Gelman, A. and Hill, J. (2007) *Data Analysis Using Regression and Multilevel/Hierarchical Models* Cambridge University Press, Cambridge.
- Gill, F.B. (1988) Trapline foraging by hermit hummingbirds: competition for an undefended, renewable resource. *Ecology*, **69**(6), 1933-1942.
- Hao, K., Tian, Z.X., Wang, Z.C., Huang, S.Q. (2020) Pollen grain size associated with pollinator feeding strategy. *Proceedings of the Royal Society B-Biological Sciences*, **287**(1933).
- Harder, L.D. (1998) Pollen-size comparisons among animal-pollinated angiosperms with different pollination characteristics. *Biological Journal of the Linnean Society*, **64**(4),

513-525.

- Harder, L.D. and Johnson, S.D. (2008) Function and evolution of aggregated pollen in angiosperms. *International Journal of Plant Sciences*, **169**(1), 59-78.
- Harder, L.D. and Thomson, J.D. (1989) Evolutionary options for maximizing pollen dispersal of animal-pollinated plants. *American Naturalist*, **133**(3), 323-344.
- Harder, L.D. and Wilson, W.G. (1994) Floral evolution and male reproductive success: optimal dispensing schedules for pollen dispersal by animal-pollinated plants. *Evolutionary Ecology*, **8**(5), 542-559.
- Harder, L.D. and Wilson, W.G. (1998) Theoretical consequences of heterogeneous transport conditions for pollen dispersal by animals. *Ecology*, **79**(8), 2789-2807.
- Harrison, X.A. (2015) A comparison of observation-level random effect and Beta-Binomial models for modelling overdispersion in Binomial data in ecology & evolution. *Peerj*, **3**.
- Harrison, X.A., Donaldson, L., Correa-Cano, M.E., Evans, J., Fisher, D.N., Goodwin, C.E., Robinson, B.S., Hodgson, D.J., Inger, R. (2018) A brief introduction to mixed effects modelling and multi-model inference in ecology. *Peerj*, **6**.
- Heisig, J.P. and Schaeffer, M. (2019) Why you should always include a random slope for the lower-level variable involved in a cross-level interaction. *European Sociological Review*, **35**(2), 258-279.
- Hemsley, A.J. and Ferguson, I.K. (1985) Pollen morphology of the genus *Erythrina* (Leguminosae: Papilionoideae) in relation to floral structure and pollinators. *Annals of the Missouri Botanical Garden*, **72**(3), 570-590.
- Hesse, M. (1981) The fine structure of the exine in relation to the stickiness of angiosperm pollen. *Review of Palaeobotany and Palynology*, **35**(1), 81-92.
- Holmquist, K.G., Mitchell, R.J., Karron, J.D. (2012) Influence of pollinator grooming on pollen-mediated gene dispersal in *Mimulus ringens* (Phrymaceae). *Plant Species*

- Biology, **27**(1), 77-85.
- Inchaussandague, M., Skigin, D., Dolinko, A., Telleria, M.C., Barreda, V.D., Palazzesi, L. (2018) Spines, microspines and electric fields: a new look at the possible significance of sculpture in pollen of basal and derived Asteraceae. *Biological Journal of the Linnean Society*, **125**(4), 794-801.
- Inouye, D.W., Gill, D.E., Dudash, M.R., Fenster, C.B. (1994) A model and lexicon for pollen fate. *American Journal of Botany*, **81**(12), 1517-1530.
- Ishii, H.S. and Sakai, S. (2001) Effects of display size and position on individual floral longevity in racemes of *Nartheicum asiaticum* (Liliaceae). *Functional Ecology*, **15**(3), 396-405.
- Kendall, D.A. and Solomon, M.E. (1973) Quantities of pollen on bodies of insects visiting apple blossom. *Journal of Applied Ecology*, **10**(2), 627-634.
- Kessler, D., Gase, K., Baldwin, I.T. (2008) Field experiments with transformed plants reveal the sense of floral scents. *Science*, **321**(5893), 1200-1202.
- Koch, L., Lunau, K., Wester, P. (2017) To be on the safe site - Ungroomed spots on the bee's body and their importance for pollination. *Plos One*, **12**(9).
- Konzmann, S., Koethe, S., Lunau, K. (2019) Pollen grain morphology is not exclusively responsible for pollen collectability in bumble bees. *Scientific Reports*, **9**.
- Korner, C. (2007) The use of 'altitude' in ecological research. *Trends in Ecology & Evolution*, **22**(11), 569-574.
- Krauss, S.L., Phillips, R.D., Karron, J.D., Johnson, S.D., Roberts, D.G., Hopper, S.D. (2017) Novel consequences of bird pollination for plant mating. *Trends in Plant Science*, **22**(5), 395-410.
- Kuriya, S., Hattori, M., Nagano, Y., Itino, T. (2015) Altitudinal flower size variation correlates with local pollinator size in a bumblebee-pollinated herb, *Prunella vulgaris* L. (Lamiaceae). *Journal of Evolutionary Biology*, **28**(10), 1761-1769.

- Lau, T.C. and Stephenson, A.G. (1993) Effects of soil nitrogen on pollen production, pollen grain size, and pollen performance in *Cucurbita pepo* (Cucurbitaceae). *American Journal of Botany*, **80**(7), 763-768.
- Lefebvre, V., Villemant, C., Fontaine, C., Daugeron, C. (2018) Altitudinal, temporal and trophic partitioning of flower-visitors in Alpine communities. *Scientific Reports*, **8**.
- Li, X.X., Wang, H., Gituru, R.W., Guo, Y.H., Yang, C.F. (2014) Pollen packaging and dispensing: adaptation of patterns of anther dehiscence and flowering traits to pollination in three *Epimedium* species. *Plant Biology*, **16**(1), 227-233.
- Lin, H., Gomez, I., Meredith, J.C. (2013) Pollenkitt wetting mechanism enables species-specific tunable pollen adhesion. *Langmuir*, **29**(9), 3012-3023.
- Lin, H.S., Qu, Z.H., Meredith, J.C. (2016) Pressure sensitive microparticle adhesion through biomimicry of the pollen-stigma interaction. *Soft Matter*, **12**(11), 2965-2975.
- Lloyd, D.G. (1983) Evolutionarily stable sex-ratios and sex allocation. *Journal of Theoretical Biology*, **105**(3), 525-539.
- Lloyd, D.G. and Yates, J.M.A. (1982) Intrasexual selection and the segregation of pollen and stigmas in hermaphrodite plants, exemplified by *Wahlenbergia albomarginata* (Campanulaceae). *Evolution*, **36**(5), 903-913.
- Lunau, K., Piorek, V., Krohn, O., Pacini, E. (2015) Just spines—mechanical defense of malvaceous pollen against collection by corbiculate bees. *Apidologie*, **46**(2), 144-149.
- Lynn, A., Piotter, E., Harrison, E., Galen, C. (2020) Sexual and natural selection on pollen morphology in *Taraxacum*. *American Journal of Botany*, **107**(2), 364-374.
- Makino, T.T., Ohashi, K., Sakai, S. (2007) How do floral display size and the density of surrounding flowers influence the likelihood of bumble bee revisitation to a plant? *Functional Ecology*, **21**(1), 87-95.
- McCabe, L.M. and Cobb, N.S. (2021) From bees to flies: Global shift in pollinator communities

- along elevation gradients. *Frontiers in Ecology and Evolution*, **8**.
- McCallum, B. and Chang, S.M. (2016) Pollen competition in style: Effects of pollen size on siring success in the hermaphroditic common morning glory, *Ipomoea purpurea*. *American Journal of Botany*, **103**(3), 460-470.
- Michener, C.D. (1999) The corbiculae of bees. *Apidologie*, **30**(1), 67-74.
- Minnaar, C., Anderson, B., de Jager, M.L., Karron, J.D. (2019) Plant-pollinator interactions along the pathway to paternity. *Annals of Botany*, **123**(2), 225-245.
- Mitchell, R.J., Wilson, W.G., Holmquist, K.G., Karron, J.D. (2013) Influence of pollen transport dynamics on sire profiles and multiple paternity in flowering plants. *Plos One*, **8**(10).
- Morris, W.F., Price, M.V., Waser, N.M., Thomson, J.D., Thomson, B., Stratton, D.A. (1994) Systematic increase in pollen carryover and its consequences for geitonogamy in plant populations. *Oikos*, **71**(3), 431-440.
- Nagano, Y., Abe, K., Kitazawa, T., Hattori, M., Hirao, A.S., Itino, T. (2014) Changes in pollinator fauna affect altitudinal variation of floral size in a bumblebee-pollinated herb. *Ecology and Evolution*, **4**(17), 3395-3407.
- Ohashi, K. and Thomson, J.D. (2009) Trapline foraging by pollinators: its ontogeny, economics and possible consequences for plants. *Annals of Botany*, **103**(9), 1365-1378.
- Ollerton, J., Winfree, R., Tarrant, S. (2011) How many flowering plants are pollinated by animals? *Oikos*, **120**(3), 321-326.
- Pacini, E. and Franchi, G.G. (2020) Pollen biodiversity - why are pollen grains different despite having the same function? A review. *Botanical Journal of the Linnean Society*, **193**(2), 141-164.
- Pacini, E. and Hesse, M. (2005) Pollenkitt—its composition, forms and functions. *Flora*, **200**(5), 399-415.
- Parker, A.J., Tran, J.L., Ison, J.L., Bai, J.D.K., Weis, A.E., Thomson, J.D. (2015) Pollen packing

- affects the function of pollen on corbiculate bees but not non-corbiculate bees. *Arthropod-Plant Interactions*, **9**(2), 197-203.
- Parker, A.J., Williams, N.M., Thomson, J.D. (2018) Geographic patterns and pollination ecotypes in *Claytonia virginica*. *Evolution*, **72**(1), 202-210.
- Pi, H.Q., Quan, Q.M., Wu, B., Lv, X.W., Shen, L.M., Huang, S.Q. (2021) Altitude-related shift of relative abundance from insect to sunbird pollination in *Elaeagnus umbellata* (Elaeagnaceae). *Journal of Systematics and Evolution*, **59**(6), 1266-1275.
- Queller, D.C. (1984) Pollen-ovule ratios and hermaphrodite sexual allocation strategies. *Evolution*, **38**(5), 1148-1151.
- Rademaker, M.C.J., deJong, T.J., Klinkhamer, P.G.L. (1997) Pollen dynamics of bumble-bee visitation on *Echium vulgare*. *Functional Ecology*, **11**(5), 554-563.
- Roquer-Beni, L., Rodrigo, A., Arnan, X., Klein, A.M., Fornoff, F., Boreux, V., Bosch, J. (2020) A novel method to measure hairiness in bees and other insect pollinators. *Ecology and Evolution*, **10**(6), 2979-2990.
- Salvatier, J., Wiecki, T.V., Fonnesbeck, C. (2016) Probabilistic programming in Python using PyMC3. *PeerJ Computer Science*, **2**.
- Sannier, J., Baker, W.J., Anstett, M.-C., Nadot, S. (2009) A comparative analysis of pollinator type and pollen ornamentation in the Araceae and the Arecaceae, two unrelated families of the monocots. *BMC Research Notes*, **2**(145).
- Sarkissian, T.S. and Harder, L.D. (2001) Direct and indirect responses to selection on pollen size in *Brassica rapa* L. *Journal of Evolutionary Biology*, **14**(3), 456-468.
- Schneider, C.A., Rasband, W.S., Eliceiri, K.W. (2012) NIH Image to ImageJ: 25 years of image analysis. *Nature Methods*, **9**(7), 671-675.
- Simpson, E.H. (1949) Measurement of diversity. *Nature*, **163**(4148), 688.
- Smith, C.C. and Fretwell, S.D. (1974) Optimal balance between size and number of offspring.

- American Naturalist, **108**(962), 499-506.
- Song, Y.P., Huang, Z.H., Huang, S.Q. (2019) Pollen aggregation by viscin threads in *Rhododendron* varies with pollinator. *New Phytologist*, **221**(2), 1150-1159.
- Stavert, J.R., Linan-Cembrano, G., Beggs, J.R., Howlett, B.G., Pattemore, D.E., Bartomeus, I. (2016) Hairiness: the missing link between pollinators and pollination. *Peerj*, **4**.
- Stroo, A. (2000) Pollen morphological evolution in bat pollinated plants. *Plant Systematics and Evolution*, **222**(1-4), 225-242.
- Suzuki, M.F. and Ohashi, K. (2014) How does a floral colour-changing species differ from its non-colour-changing congener? - a comparison of trait combinations and their effects on pollination. *Functional Ecology*, **28**(3), 549-560.
- Tanaka, N., Uehara, K., Murata, A. (2004) Correlation between pollen morphology and pollination mechanisms in the Hydrocharitaceae. *Journal of Plant Research*, **117**(4), 265-276.
- Tashi, S., Singh, B., Keitel, C., Adams, M. (2016) Soil carbon and nitrogen stocks in forests along an altitudinal gradient in the eastern Himalayas and a meta-analysis of global data. *Global Change Biology*, **22**(6), 2255-2268.
- Thomson, J.D. (1986) Pollen transport and deposition by bumble bees in *Erythronium*: influences of floral nectar and bee grooming. *Journal of Ecology*, **74**(2), 329-341.
- Thomson, J.D., Maddison, W.P., Plowright, R.C. (1982) Behavior of bumble bee pollinators of *Aralia hispida* Vent. (Araliaceae). *Oecologia*, **54**(3), 326-336.
- Thorp, R.W. (1979) Structural, behavioral, and physiological adaptations of bees (Apoidea) for collecting pollen. *Annals of the Missouri Botanical Garden*, **66**(4), 788-812.
- Thorp, R.W. (2000) The collection of pollen by bees. *Plant Systematics and Evolution*, **222**(1-4), 211-223.
- Toji, T., Ishimoto, N., Egawa, S., Nakase, Y., Hattori, M., Itino, T. (2021) Intraspecific

- convergence of floral size correlates with pollinator size on different mountains: a case study of a bumblebee-pollinated *Lamium* (Lamiaceae) flowers in Japan. *Bmc Ecology and Evolution*, **21**(1).
- Tong, Z.Y. and Huang, S.Q. (2018) Safe sites of pollen placement: a conflict of interest between plants and bees? *Oecologia*, **186**(1), 163-171.
- Vaissière, B.E. and Vinson, S.B. (1994) Pollen morphology and its effect on pollen collection by honey bees, *Apis mellifera* L. (Hymenoptera: Apidae), with special reference to upland cotton, *Gossypium hirsutum* L. (Malvaceae). *Grana*, **33**(3), 128-138.
- Vonhof, M.J. and Harder, L.D. (1995) Size-number trade-offs and pollen production by papilionaceous legumes. *American Journal of Botany*, **82**(2), 230-238.
- Wang, G., Chen, J., Li, Z.B., Zhang, F.P., Yang, D.R. (2014) Has pollination mode shaped the evolution of *Ficus* pollen? *Plos One*, **9**(1).
- Wang, L.L., Zhang, C., Yang, M.L., Zhang, G.P., Zhang, Z.Q., Yang, Y.P., Duan, Y.W. (2017) Intensified wind pollination mediated by pollen dimorphism after range expansion in an ambophilous biennial *Aconitum gymnantrum*. *Ecology and Evolution*, **7**(2), 541-549.
- Warren, S.D., Harper, K.T., Booth, G.M. (1988) Elevational distribution of insect pollinators. *American Midland Naturalist*, **120**(2), 325-330.
- Welsford, M.R., Hobbhahn, N., Midgley, J.J., Johnson, S.D. (2016) Floral trait evolution associated with shifts between insect and wind pollination in the dioecious genus *Leucadendron* (Proteaceae). *Evolution*, **70**(1), 126-139.
- Willmer, P. (2011) *Pollination and Floral Ecology* Princeton University Press, Princeton.
- Wolfram Research (2017) *Mathematica* Wolfram Research Inc., Champaign, Illinois.